NATIONAL ADVISORY COMMITTEE FOR AERONAUTICS

TECHNICAL NOTE 4336

EXPERIMENTAL INVESTIGATION OF AXIAL AND NORMAL FORCE CHARACTERISTICS OF SKEWED NOZZLES

By David J. Carter, Jr., and Allen R. Vick

Langley Aeronautical Laboratory
Langley Field, Va.

Washington

September 1958

NATIONAL ADVISORY COMMITTEE FOR AERONAUTI

TECHNICAL NOTE 4336

EXPERIMENTAL INVESTIGATION OF AXIAL AND NORMAL FORCE CHARACTERISTICS OF SKEWED NOZZLES

By David J. Carter, Jr., and Allen R. Vick

SUMMARY

An investigation of normal forces produced by several "skewed" nozzles and a series of ejectors with skewed shrouds discharging into quiescent air has been conducted with cold air at jet total-pressure ratios up to 6.5. Nozzles were terminated at angles of 30°, 45°, 60°, and 75° relative to the normal plane. Ejector nozzles consisting of 60° skewed shrouds surrounding either an axisymmetric primary nozzle or a 60° skewed primary nozzle were tested at diameter ratios from 1.05 to 1.45 and spacing ratios from 0.5 to 2.87. Stagnation pressure of the induced secondary flow was equal to the ambient pressure.

Normal forces developed on nozzles skewed at least 45° increased to 25 percent of the axial thrust as the pressure ratio was increased to 6.5; these normal forces were produced with no apparent loss in axial thrust relative to the unskewed (sonic) nozzle. Strict agreement with the cosine law is maintained, however, because a skewed nozzle allows the flow to expand within the nozzle, increasing its velocity and hence the resultant thrust. Ejectors with sonic primaries developed normal forces which generally decreased with increasing diameter ratio but were not significantly affected by variation in spacing ratio within the range of these tests. Normal forces developed on ejectors with skewed primary nozzles were less than those developed on the primary nozzle alone; exceptions occurred with the ejectors of largest diameter ratio and smallest spacing ratio, which permitted the deflected primary jet to exhaust without interference from the secondary shroud.

INTRODUCTION

Jet-deflecting devices are being used on several current airplanes and missiles and are being considered for many new designs. On wing-mounted nacelles these devices can add appreciable lift to shorten the take-off run or to improve lift-drag ratios at high Mach numbers. A jet or reaction type of control is needed for VTOL and STOL aircraft and for high-altitude vehicles because of the ineffectiveness of aerodynamic control surfaces when the dynamic pressure approaches zero.

Tests of several devices in which jet deflection has been achieved by elbows or vanes have been reported. (See refs. 1 to 3.) Other tests of nozzles which were terminated in planes oblique to the nozzle axis have shown significant jet deflection when operating above the design pressure ratio (ref. 4). These skewed nozzles were of square cross section.

In the present investigation the skewed-nozzle principle has been applied to nozzles of circular cross section. Since most current engines require tailpipe cooling which is generally accomplished by use of ejector nozzles, several ejector configurations also have been tested. These included configurations with skewed primary and secondary nozzles as well as those in which only the secondary shroud was skewed. Normal and axial force components of these nozzles exhausting into quiescent air were measured at jet pressure ratios up to 6.5. In the ejector tests the stagnation pressure of the secondary flow was equal to the ambient pressure. Measured axial thrusts are compared with the ideal thrust of a variable supersonic nozzle; the normal force on the simple skewed nozzles is compared with the values calculated from two-dimensional considerations.

SYMBOLS

A	area, sq in.
D	internal diameter, in.
$\frac{D_s}{D_p}$	ratio of secondary diameter to primary diameter
F_n	normal force, lb
$\frac{F_n}{T_a}$	normal-force ratio
h	height of indentation (fig. 2)
m	mass flow, slugs/sec
$\frac{m_s}{m_p}$	ejector mass-flow ratio
p	static pressure, lb/sq in.

p_t	total pressure, lb/sq in.
$\frac{p_{t,j}}{p_{am}}$	nozzle pressure ratio
q	dynamic pressure, $\frac{1}{2}\rho V^2$, lb/sq in.
S	shroud length measured along axis, in.
$\frac{S}{D_p}$	spacing ratio
T	thrust, lb
T_a	measured axial thrust
T_i	ideal axial thrust for a variable supersonic nozzle
$\frac{T_a}{T_i}$	axial-thrust ratio
V	velocity, ft/sec
x	distance from throat along extended lip
θ	nozzle-exit angle relative to plane normal to axis
ρ	density, slugs/cu ft

Subscripts:

a	axial (measured value)
am	ambient
i	theoretical ideal
j	jet
n	normal or perpendicular
p	primary
s	secondary

th throat conditions

u unskewed (i.e., exit plane perpendicular to the axis)

APPARATUS AND PROCEDURE

Figure 1 shows the general arrangement of the L-shaped test setup. Air stored in outside tanks at 100 pounds per square inch gage permitted continuous testing for 15 minutes at pressures on the order of 80 pounds per square inch gage. This air entered the L-shaped test arm through a series of valves and a 6- to 3-inch reducer. The vertical support leg and elbow of the test arm were 3 inches in diameter; the horizontal arm was 1.5-inch (inside diameter) steel tubing at the end of which the 1-inch (inside diameter) test nozzles were attached. The test arm was instrumented to enable simultaneous measurement of the normal force and the axial force exerted on the nozzle. Deflection of the horizontal arm provided measurement of the normal force while deflection of the vertical leg indicated the axial thrust. The deflections were measured by unbonded strain gages with maximum deflection of ±0.0015 inch. Two strain gages were mounted on opposite sides of the vertical leg, and one gage was used to measure deflections of the horizontal arm. The stagnation pressure in the reducer was measured with a calibrated pressure cell. The outputs of the force gages and pressure cell were continuously recorded by electronic function plotters (three-variable recording potentiometers).

Normal-force measurements were not affected by the axial-thrust component since the support arm for the normal-force gage remained stationary relative to the unloaded position of the horizontal arm. However, normal forces on the horizontal arm contributed to the indicated axial thrust. Consequently, the axial-thrust gages were calibrated under various normal-load conditions, and a calibration factor was applied to the measured values of axial thrust. Since the center of pressure varied with jet total-pressure ratio and angle of skew, the horizontal arm was calibrated for several loading positions along the nozzle lip. Maximum variation in center of pressure from the mean value resulted in possible errors of ±2 percent of the normal force.

Stagnation-pressure losses in the system were determined by a survey across the exit of a sonic test nozzle. The ratio of the mean stagnation pressure at the nozzle exit to the measured value at the reducer was 0.975; the data were corrected accordingly during computations. Secondary mass-flow rates were determined from static pressures measured at four equally spaced positions around the skewed shroud and recorded from a multiple-tube manometer. The mass-flow ratios m_s/m_p plotted in the

figures represent the ratio of the measured secondary flow to the measured flow from the primary nozzle.

A double-pass coincident schlieren system was used for photographing exhaust shock patterns. Schlieren pictures were taken in a separate series of tests rather than during the force-measurement tests.

Because the jet air was stored in outside tanks, its temperature often differed significantly from that of the setup located indoors. To minimize the effects of temperature changes during the tests, two axial-thrust gages were electrically connected to compensate for expansions and contractions, and air was passed through the setup until temperature equilibrium was established. Data obtained with this arrangement and procedure had possible inaccuracies in normal-force ratio F_n/T_a not exceeding ± 0.01 at the higher loading conditions.

Sketches showing the configurations of the nozzles tested are presented in figure 2. In the column headed "Skewed nozzles" two basic configurations are shown; dashed lines indicate alterations investigated. The top sketch shows a skewed nozzle with variation in angle of skew; below it is shown a 60° skewed nozzle with variation in the amount of indentation. In the middle column ejector configurations with 60° skewed shrouds and unskewed primary nozzles are shown for diameter ratios from 1.05 to 1.45; the last column shows the three largest shrouds with a 60° skewed primary nozzle. Changes in spacing ratio were accomplished by shortening the shrouds.

CALCULATED PERFORMANCE

In order to furnish a reference from which to evaluate the measured results, theoretical force components are presented in figures 3 and 4. Normal forces were calculated from two-dimensional concepts and axial thrust was determined from momentum considerations.

The normal force characteristics (force perpendicular to nozzle axis) of two-dimensional skewed nozzles, calculated by the method of characteristics for jet pressure ratios up to 6.85, are presented in figure 3. These were determined from calculated pressure distributions along the extended lip. These calculations were based on the assumption of a Prandtl-Meyer expansion originating at the upstream edge of the nozzle exit and expanding to an ambient pressure of 14.7 pounds per square inch absolute. A typical pressure distribution along the extended lip is shown in the lower insert in figure 3. In carrying out these calculations, it has been assumed that the flow would expand until a minimum pressure, equal to two-thirds the ambient value, was reached; at this point separation would occur and the pressure at all points farther

downstream was considered equal to the ambient. As skew angle increases (increasing lip length L) the normal force is shown to increase steadily to a maximum value, which is a function of jet pressure ratio. The lip length for which this maximum normal force occurs corresponds to the value of θ for which the pressure at the downstream edge of the nozzle lip reaches the ambient pressure (see typical pressure distribution). Further increases in θ cause a reduction in normal force. This reduction is produced by subambient pressures acting on that portion of the lip extending beyond the optimum length. Since ambient pressure is assumed downstream of the separation point, the normal force remains constant as θ is increased further. At a constant skew angle, normal force increases with pressure ratio because of the increase in static pressures along the lip and also because of the increased lip area subjected to greater than ambient pressures. The optimum angle of skew increases with jet pressure ratio.

Calculated axial thrust for both an unskewed nozzle and an ideal supersonic nozzle are presented in figure 4 as a function of pressure ratio. (An ideal supersonic nozzle is defined as one in which the air is expanded to ambient pressure at the exit plane.) Curves for both nozzles are essentially linear, with the ideal nozzle producing more axial thrust at the higher pressure ratios. The ratio of the theoretical thrusts is indicated at the top of the figure along with typical values from tests of an unskewed (sonic) nozzle, which are presented for comparison. The measured thrust ratios were about 0.95 at the lower pressures and decreased to about 0.93 at a pressure ratio of 6.

RESULTS AND DISCUSSION

The basic data of this investigation of skewed nozzles and of ejectors with skewed shrouds discharging into quiescent air are presented together with schlieren photographs in figures 5 to 13. Following the basic-data presentation are summary plots of normal force characteristics for each series of models tested (figs. 14 to 20). Although the principal aim of this investigation was the determination of normal forces developed by these nozzles, axial thrust was also measured, and in the case of the ejectors, the secondary mass flow. All three parameters have been presented in nondimensional form $\left(m_s/m_p,\ T_a/T_j,\ \text{and}\ F_n/T_a\right)$ as functions of primary jet total-pressure ratio $\left(p_{t,j}/p_{am}\right)$. In preliminary tests of 60° skewed nozzles, experimental data indicated that a wall thickness of 0.025 inch to 0.15 inch had negligible effect on the normal force characteristics. Consequently, the wall thickness of all other nozzles and shrouds reported in this investigation was fixed at 0.025 inch.

Basic Data

In figure 5(a), the normal force characteristics of four simple skewed nozzles are compared with results calculated by two-dimensional theory. The agreement is surprisingly good in view of the fact that this two-dimensional theory represents such a gross simplification of the true flow picture. Also shown in this figure are several data points taken from tests of nozzles with square cross sections (ref. 4). These results, too, show fair agreement with the calculations even though the effects of the finite nozzle width were neglected by theory. The axial thrust of the skewed circular nozzles, shown in the upper part of each diagram, varied narrowly about a value of 0.95 for these pressure ratios. The corresponding schlieren photographs, presented on figure 5(b), are arranged in four groups orientated in the same pattern as the data figures. Within each group the pictures are so arranged that similar pressure ratios appear in the same relative position. In general, the photographs show increasing jet deflection with increasing pressure ratio; the jet was considerably more diffused at the larger angles of skew.

The force characteristics of the indented skewed nozzles ($\theta = 60^\circ$) are presented in figure 6(a) and the corresponding schlieren photographs in figure 6(b). As with the simple skewed nozzles, the normal force increased with jet pressure ratio and with increasing lip extension. The axial-thrust ratio decreased slightly with increasing jet pressure ratio. Again, spreading of the jet increased with lip extension.

Basic data from tests of the ejector models are presented in figures 7 to 13. The data of figure 7(a) were obtained in tests of a limiting configuration, one in which the secondary shroud fitted snugly over the primary nozzle. For this configuration no secondary flow was possible. Because of the increase in area between the primary throat and the shroud exit, this nozzle might be considered to have a supersonic design Mach number and will therefore have lower pressures along the extended lip. A corresponding loss in normal force is indicated by the data. The axial thrust of these configurations was slightly higher than that of the simple nozzles of figure 5(a), especially at the higher pressure ratios. The schlieren photographs showed changes in the shock patterns as the spacing ratio was increased from 1 to 1.55. However, differences in jet deflection between these nozzles and the 60° skewed nozzles of figure 5(b) are not apparent.

In presenting the characteristics of ejector configurations with unskewed primary nozzles (figs. 8 to 10) curves of the secondary mass-flow ratio are shown, along with force data. In general the secondary flow was highest at low pressure ratios and decreased with increasing $p_{t,j}/p_{am}$. This reduction occurred as the primary jet, expanding with increased pressure, reduced the effective area of the secondary passage.

The secondary flow reached zero at a pressure ratio which was dependent upon the area ratio of the ejector. The axial-thrust characteristics of these models were generally similar to those of the simple nozzles. However, the normal force was often slightly negative at the lower pressure ratios. This is consistent with the downward deflection of the jet shown in several of the schlieren photographs. As in the simple nozzle configurations, positive forces were accompanied by upward deflection of the jet.

Data from tests of ejectors with skewed primary nozzles are presented in figures 11, 12, and 13. The ratios of secondary to primary mass flow and the axial-thrust ratios of these configurations were generally similar to those of ejector models discussed previously; however, the normal forces showed significant variations which will be discussed in detail with summary plots.

Effect of Skew Angle and Indentation

The normal force characteristics of simple skewed nozzles are summarized in figure 14. At the highest pressure ratio tested, 6.5, the nozzles with 45°, 60°, and 75° angles of skew developed normal forces of 25 to 28 percent of the available axial thrust, while only 17 percent was developed by the 30° nozzle. The 30° nozzle was superior at jet pressure ratios from 1.9 to 2.8; between $p_{t,j}/p_{am}$ of 2.8 and 4.8, the 45° nozzle developed the greatest normal-force ratio, and from 4.8 to the limiting pressure ratio of these tests the 60° nozzle was best. This corroborates the calculated results (fig. 3) which indicated that the optimum angle of skew increased with pressure ratio. Because the lip extension upon which these normal forces were developed was parallel to the nozzle axis, no apparent loss in axial thrust relative to that of the unskewed nozzle occurred. The resultant thrust of the skewed nozzle was therefore greater than that of the unskewed model. This does not violate the cosine law, however, since a skewed nozzle allows the jet to expand asymmetrically within the nozzle, thereby increasing its velocity and hence the resultant thrust.

The effects of indenting the 60° skewed nozzle are shown in the summary plots in figure 15. The nozzle with $h/D = 0.2$ developed greater normal-force ratios than the unaltered skewed nozzle throughout the range of pressure ratios tested, with the greatest gain occurring near $p_{t,j}/p_{am}$ of 3.5. This gain in normal force resulted from reduction or elimination of negative forces which acted on the surface represented by the shaded areas in figure 15, where the pressures were superambient, and along the tip of the extended lip where subambient pressures often occurred. An indentation of $h/D = 0.4$ increased normal-force ratios compared with the unaltered nozzle up to pressure ratios near 4.0. Above $p_{t,j}/p_{am}$ of 4.0, the 0.4 indentation resulted in a loss in the

normal force because of the reduced lip extension. An indentation of $h/D = 0.6$ resulted in considerable reductions of the normal-force ratio. Again, the normal forces were obtained without loss in axial thrust relative to the thrust of an unskewed nozzle.

Effect of a Skewed Shroud

The normal-force characteristics of ejectors as functions of jet pressure ratio are summarized in figures 16 and 17. In figure 16, variations in normal-force ratios are shown for ejectors of several diameter ratios which had unskewed primary nozzles. At low pressure ratios where normal forces were negligible or small, no significant effect of variation in diameter ratio was observed. As the pressure ratio was increased, substantial normal forces were measured, the ejector with the smallest diameter ratio developing the greatest normal forces. As diameter ratio was increased, normal-force ratios decreased significantly. For the condition where substantial normal forces were achieved, the secondary flow was eliminated by the expanded primary jet; thus the possible advantage of cooling generally obtained with secondary flow was also eliminated. In comparison with simple skewed nozzles, these ejectors had lower normal forces at comparable pressure ratios and slight losses in axial thrust.

In figure 17, a similar comparison is shown for ejectors with skewed primary nozzles. Curves at the top of the figure show relatively high normal-force ratios. For the ejectors of larger diameter ratio, the curves are identical to those of the simple 60° skewed nozzle of figure 5. This is as might be expected, since for these configurations normal force was developed only on the primary nozzle. However, at the higher pressure ratios the secondary shroud of the ejector with diameter ratio of 1.15 interfered with the deflected primary jet and reduced the normal force. Shroud interference with the primary jet at spacing ratios of 1.0 and 1.5 introduced considerable irregularity into the normal-force curves. Wherever the primary jet impinged on the upstream lip of the shroud, forces opposing those on the primary nozzle occurred. This interference occurred first for the ejector of smallest diameter ratio at low pressure ratios. As diameter ratio increased the interference was restricted to the higher pressure ratios. It is evident that as the primary jet deflected more and more with increasing pressure ratio, the negative forces resulting from interference became greater. However, as pressure ratio and spacing ratio increased, a condition was reached where the primary jet expanded to fill the shroud (as in the case of the ejectors with unskewed primary nozzles) and positive normal components were produced on the extended lip of the skewed shroud. Thus, curves for the two models of smaller diameter ratio have a second minimum beyond which further increases in $p_{t,j}/p_{am}$ yield steadily increasing normal forces.

For the models on which the largest normal forces were measured, the secondary mass-flow ratio was relatively constant over the range of the tests.

Variations of normal force as a function of spacing ratio are presented in figures 18, 19, and 20 for ejectors with diameter ratios of 1.15, 1.25, and 1.45, respectively. With unskewed primary nozzles, the normal-force ratio at the lower jet pressure ratios varied less than 2 percent from the mean over the range of spacing ratios investigated. With ejectors having skewed primary nozzles, variation in spacing ratio caused small changes in normal force at the lowest jet pressures. But at the higher pressure ratios the normal-force ratios decreased rapidly with increasing spacing ratio until a minimum was reached; beyond this point the normal forces increased with spacing ratio as a result of increased loading of the shroud. For the ejector of largest diameter ratio, this minimum would occur beyond the range of spacing ratios tested. In general, the normal forces developed on the ejector models were less than those developed on the skewed primary alone; exceptions occurred with those ejectors of very large diameter ratio or small spacing ratio which permitted the primary jet to be exhausted without interference from the secondary shroud.

SUMMARY OF RESULTS

The results of this investigation of skewed nozzles and ejectors with skewed shrouds discharging into quiescent air are summarized as follows:

1. Normal forces developed on simple skewed nozzles of circular cross section were approximately the same as those calculated by two-dimensional theory.

2. Normal forces up to 25 percent of the axial thrust were readily produced by skewed nozzles at jet pressure ratios as low as 6.5. The angle of skew for which a nozzle produced maximum normal force increased as jet pressure ratio increased.

3. These normal forces were produced with no apparent loss in axial thrust relative to the thrust of an unskewed (sonic) nozzle. This does not represent a violation of the cosine law, however, since a skewed nozzle allows the jet to expand within the nozzle, increasing its velocity and hence the resultant thrust.

4. Indentations of a 60° skewed nozzle to two-tenths of the diameter increased the normal-force ratio throughout the range of pressure ratios

tested, whereas greater indentations resulted in significant losses at the higher pressure ratios.

5. Normal forces of significant magnitude which were developed by ejectors with unskewed primary nozzles surrounded by 60° skewed shrouds were limited to the smaller diameter ratios and the higher pressure ratios. Increasing the ejector diameter ratio resulted in lower normal forces.

6. For ejector configurations consisting of 60° skewed primary and secondary nozzles the normal forces developed were generally less than those developed on the skewed primary alone; exceptions occurred with those ejectors of very large diameter ratio or small spacing ratio which permitted the primary jet to be exhausted without interference from the secondary shroud.

Langley Aeronautical Laboratory,
National Advisory Committee for Aeronautics,
Langley Field, Va., May 26, 1958.

REFERENCES

1. McArdle, Jack G.: Internal Characteristics and Performance of Several Jet Deflectors at Primary-Nozzle Pressure Ratios up to 3.0. NACA TN 4264, 1958.

2. Von Glahn, Uwe H., and Povolny, John H.: Considerations of Some Jet-Deflection Principles for Directional Control and for Lift. Preprint No. 219, SAE National Aeronautic Meeting, Sept. 30 - Oct. 5, 1957.

3. Valerino, Alfred S.: Static Investigation of Several Jet Deflectors for Longitudinal Control of an Aircraft. NACA RM E55D04, 1955.

4. Wewerka, A., and Schmidt, H.: Investigation of Laval Nozzles and Mouths. HEC 572 (German Aero. Res. Rep. 1409), Halstead Exploiting Centre, 1941. (Available as ATI No. 27039.)

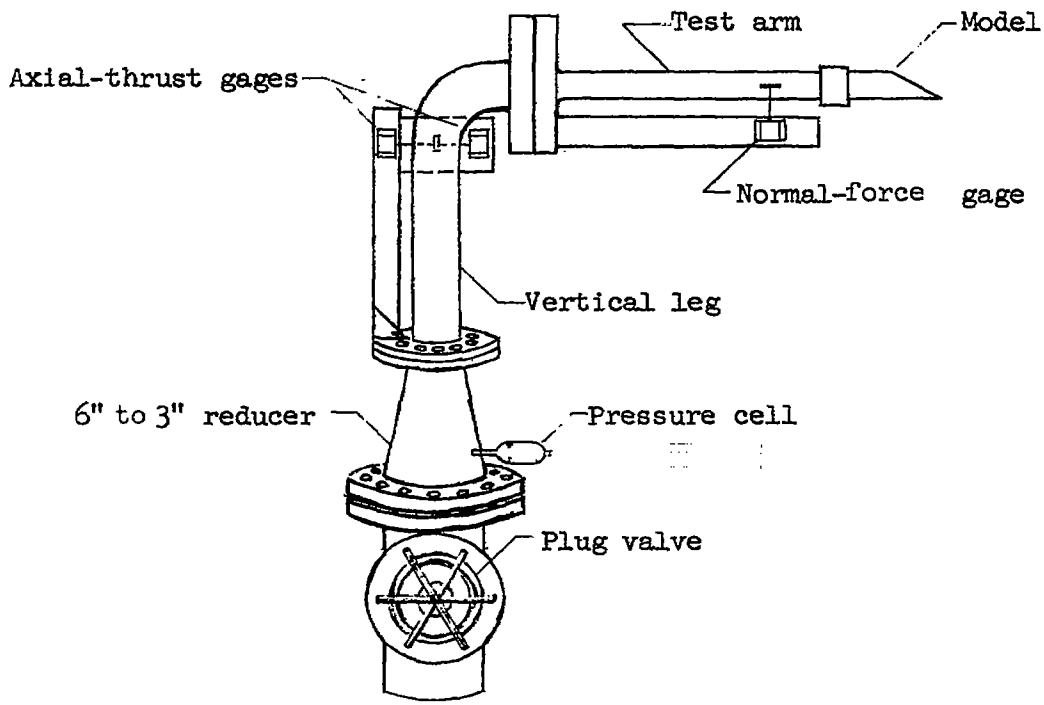

Figure 1.- L-shaped test setup.

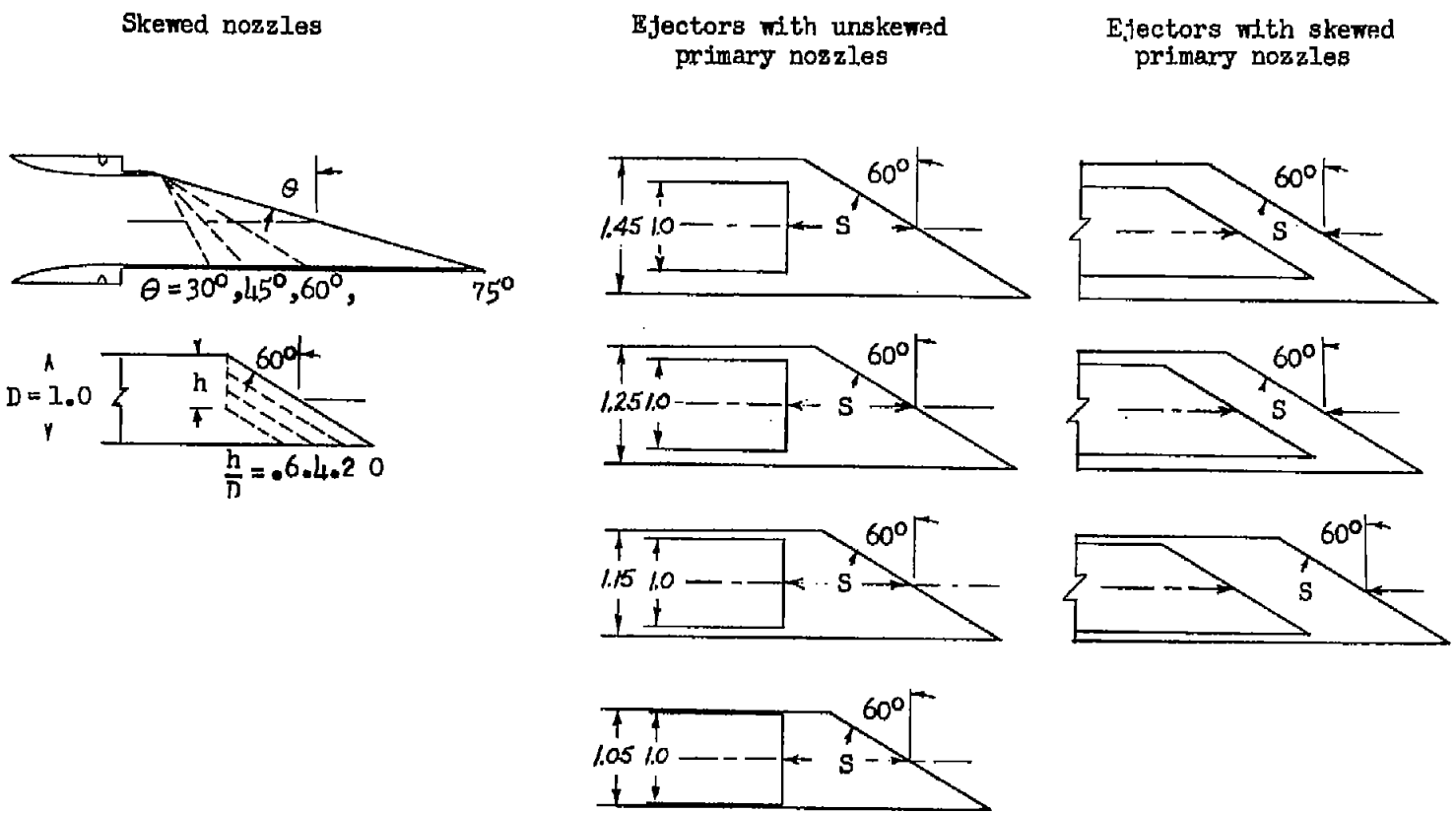

Figure 2.- Sketches of skewed nozzles and ejectors tested. Dashed lines indicate alterations.

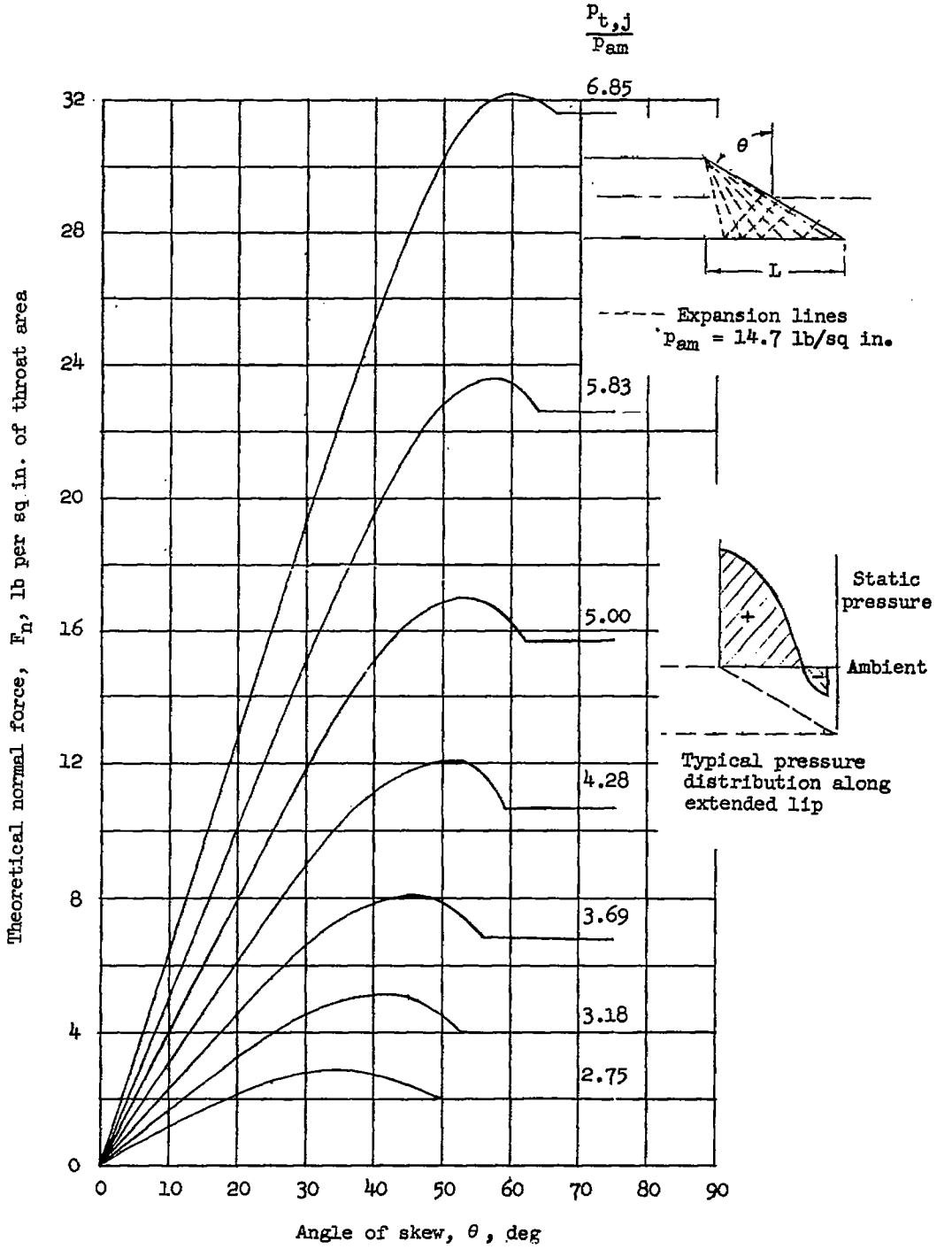

Figure 3.- Theoretical two-dimensional normal force as a function of angle of skew for pressure ratios up to 6.85.

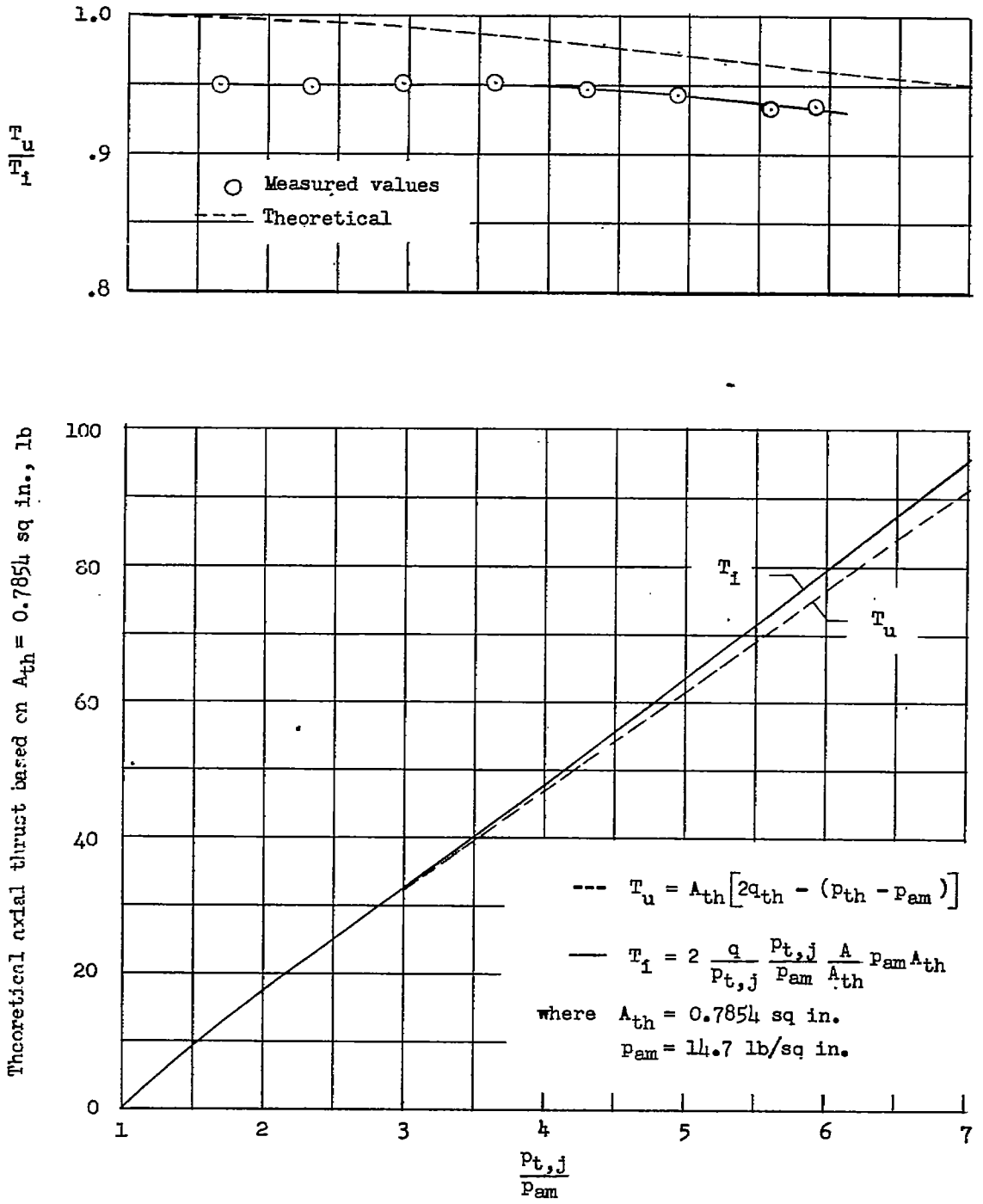

Figure 4.- Theoretical axial thrust for an unskewed nozzle and an ideal supersonic nozzle as a function of pressure ratio.

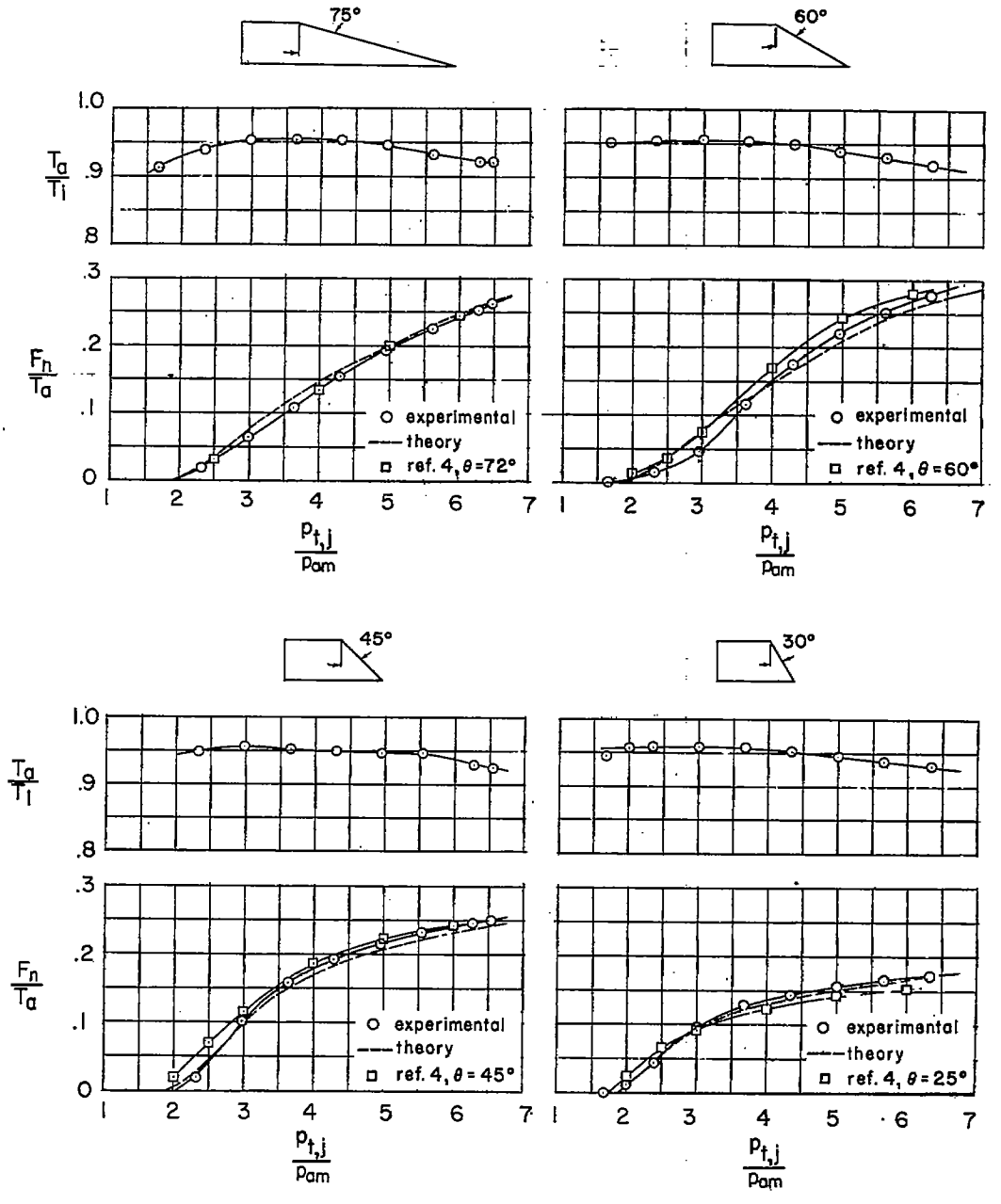

(a) Variation of T_a/T_i and F_n/T_a with $p_{t,j}/p_{am}$. Comparison is shown with two-dimensional theory and also with values taken from reference 4.

Figure 5.- Nozzles with skew angles of 75°, 60°, 45°, and 30°.

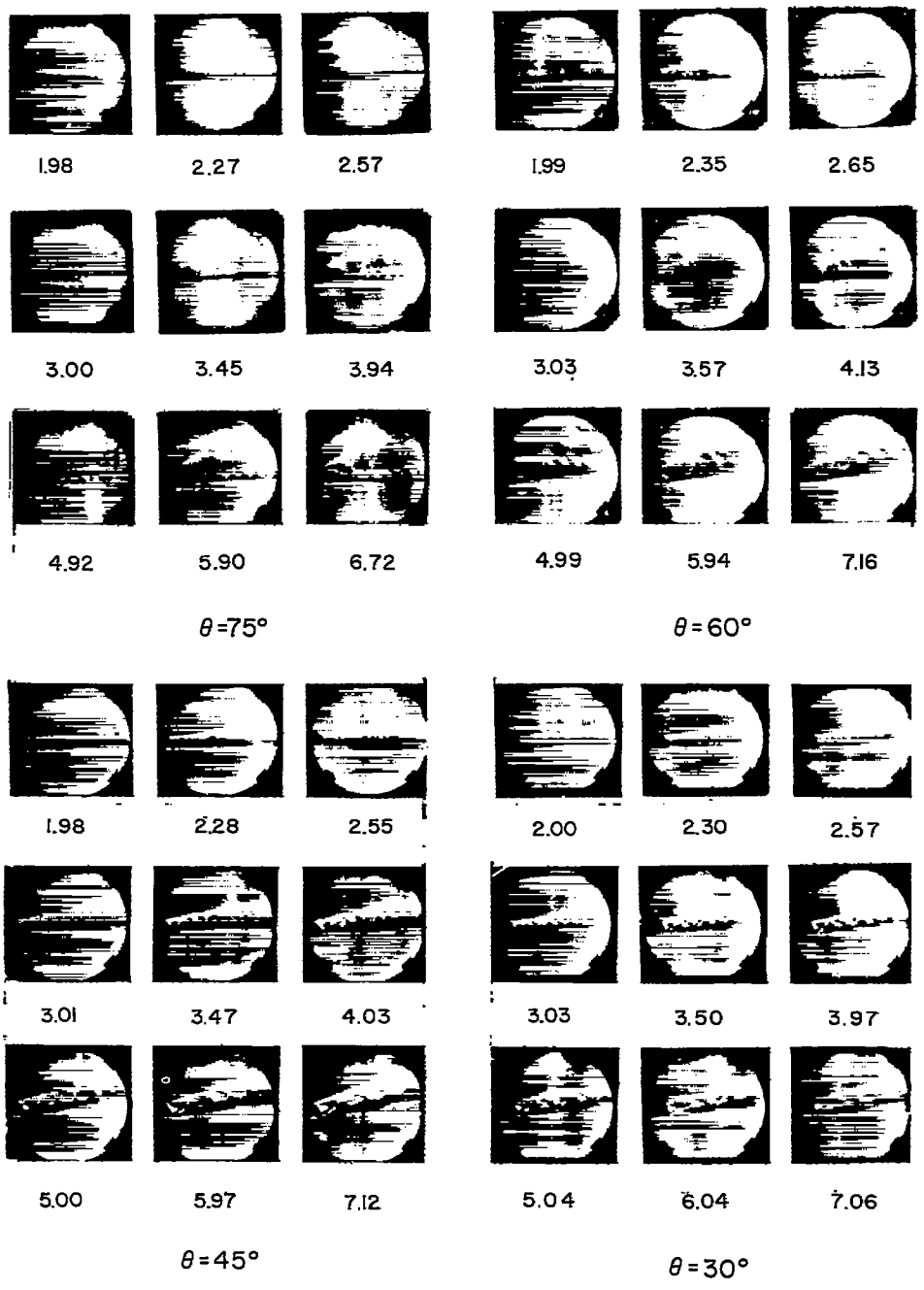

L-58-1679

(b) Schlieren photographs. Jet pressure ratio $p_{t,j}/p_{am}$ is indicated under each picture.

Figure 5.- Concluded.

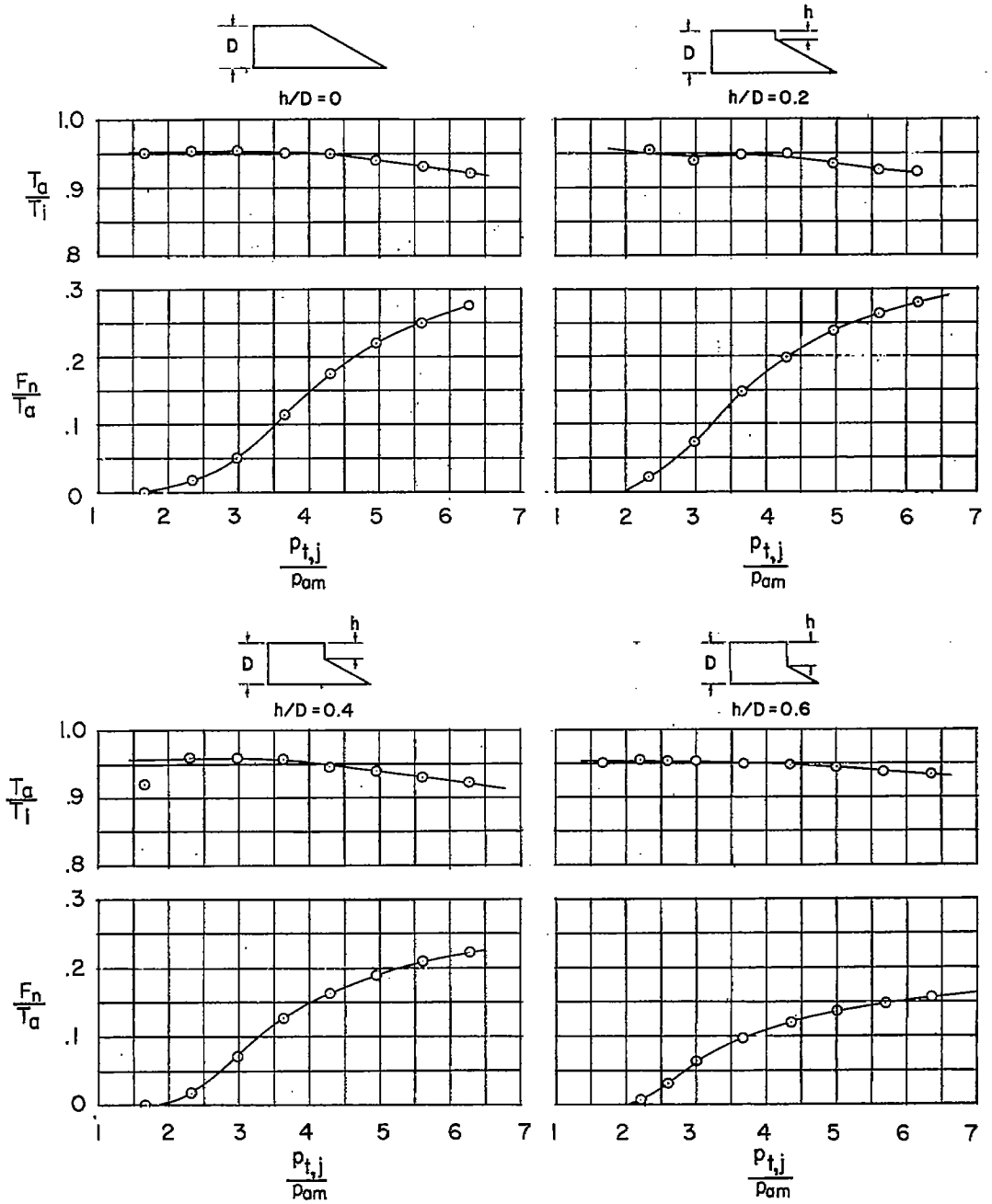

(a) Variation of T_a/T_i and F_n/T_a with $p_{t,j}/p_{am}$.

Figure 6.- 60° skewed nozzles with indentations h/D of 0, 0.2, 0.4, and 0.6.

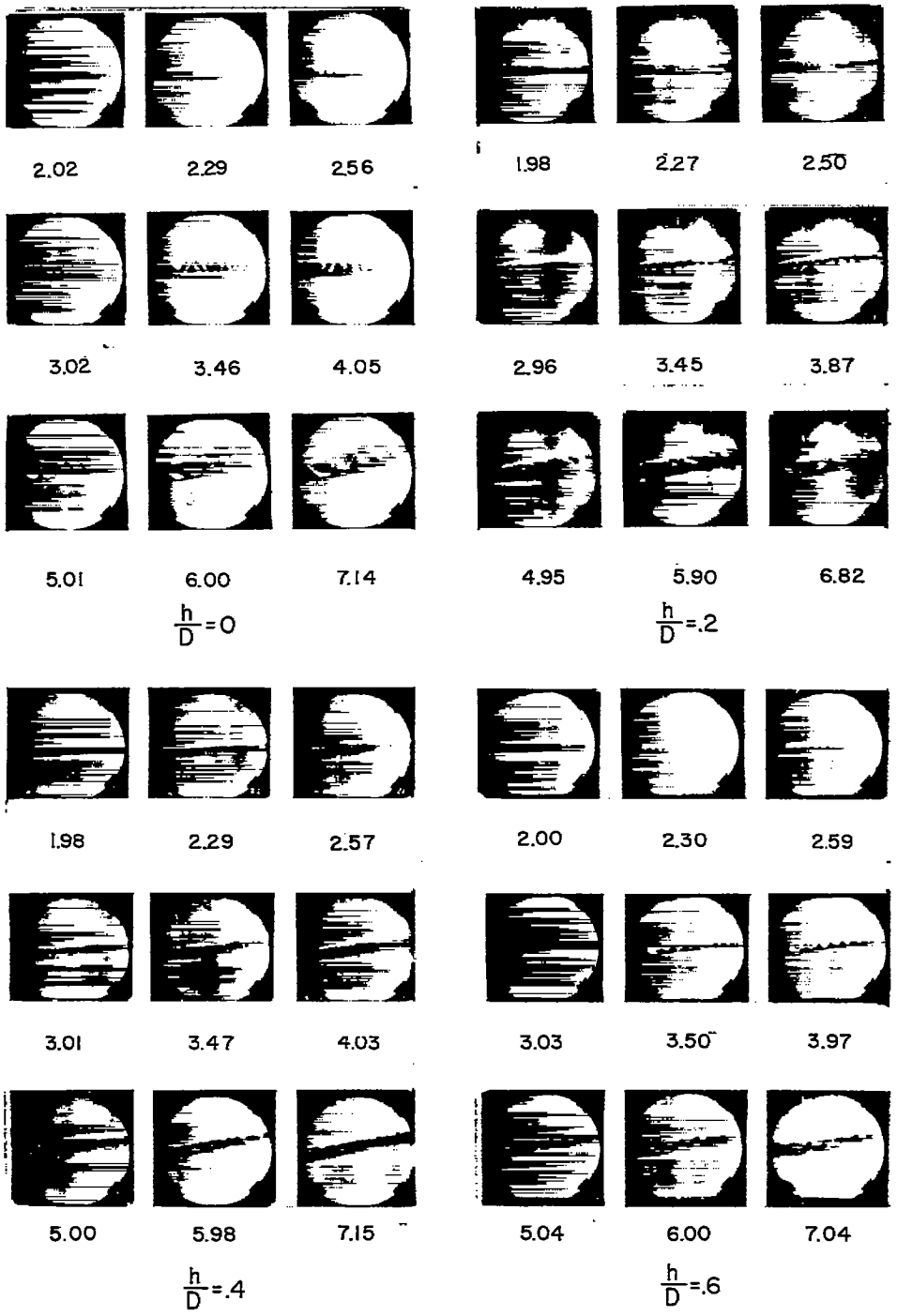

L-58-1680

(b) Schlieren photographs. Jet pressure ratio $p_{t,j}/p_{am}$ is indicated under each picture.

Figure 6.- Concluded.

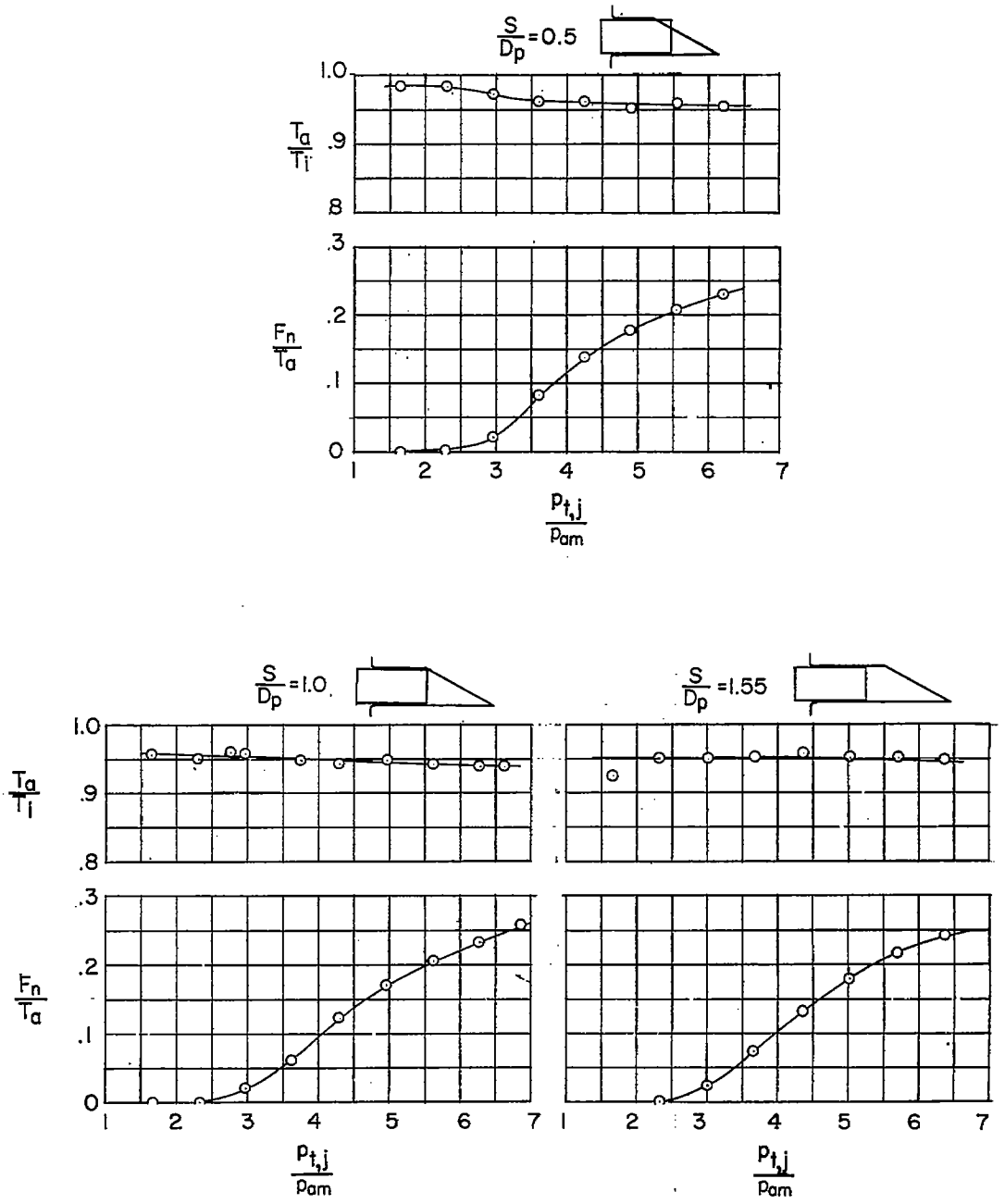

(a) Variation of T_a/T_i and F_n/T_a with $p_{t,j}/p_{am}$.

Figure 7.- Ejectors with diameter ratio of 1.05 and unskewed primary nozzles. Shroud skew angle, 60°.

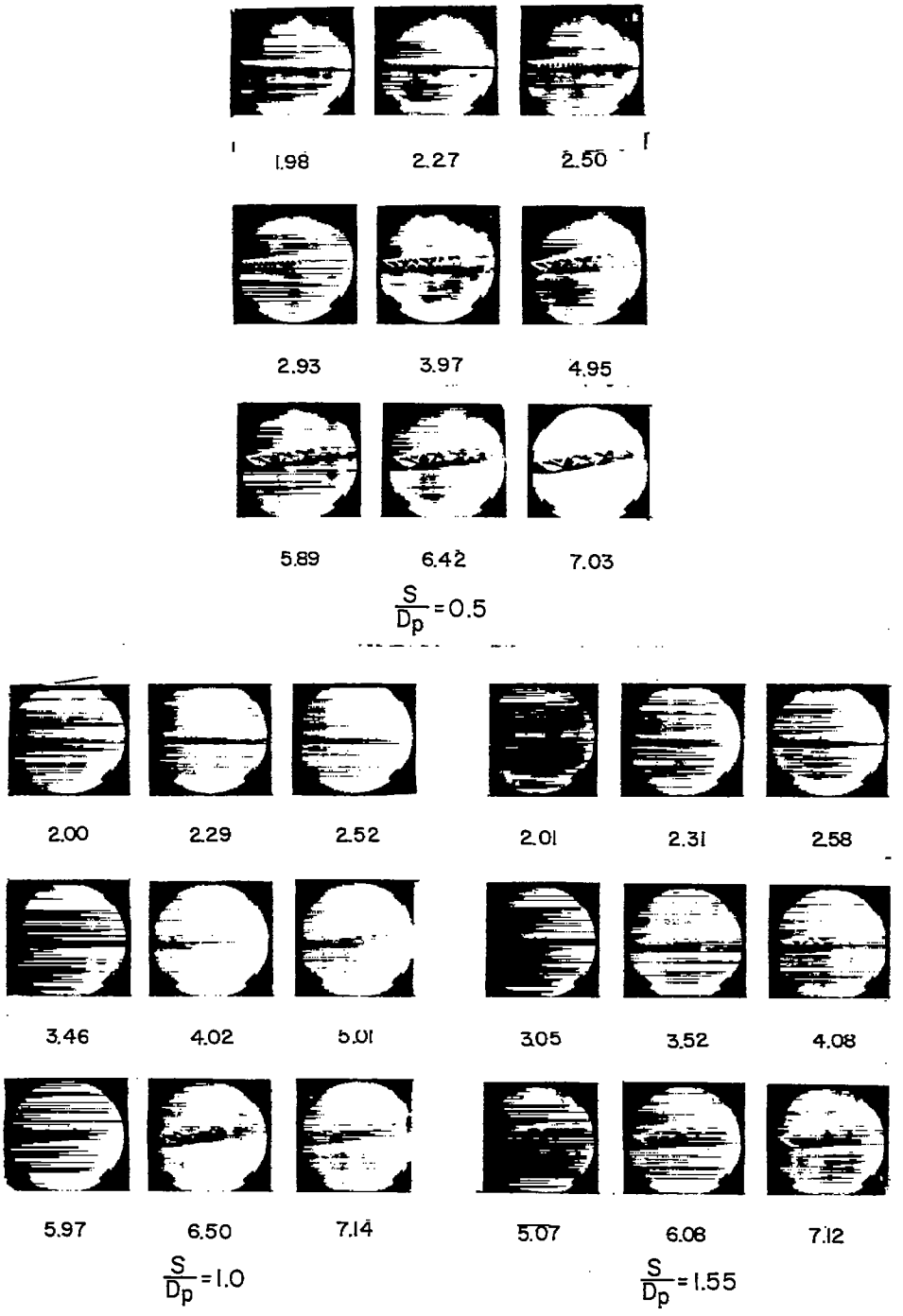

L-58-1681

(b) Schlieren photographs. Jet pressure ratio $p_{t,j}/p_{am}$ is indicated under each picture.

Figure 7.- Concluded.

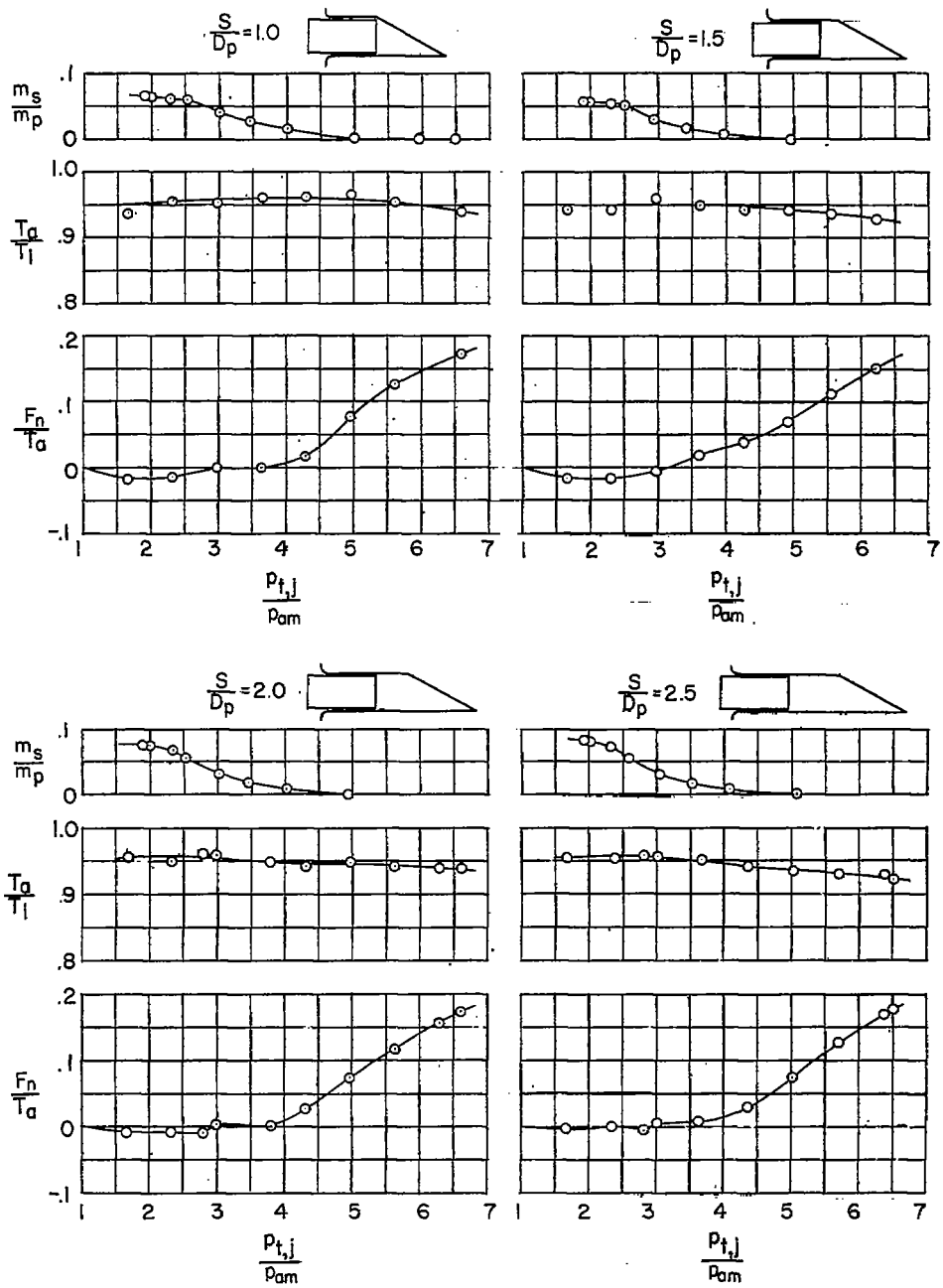

(a) Variation of m_s/m_p, T_a/T_i, and F_n/T_a with $p_{t,j}/p_{am}$.

Figure 8.- Ejectors with diameter ratio of 1.15 and unskewed primary nozzles. Shroud skew angle, 60°.

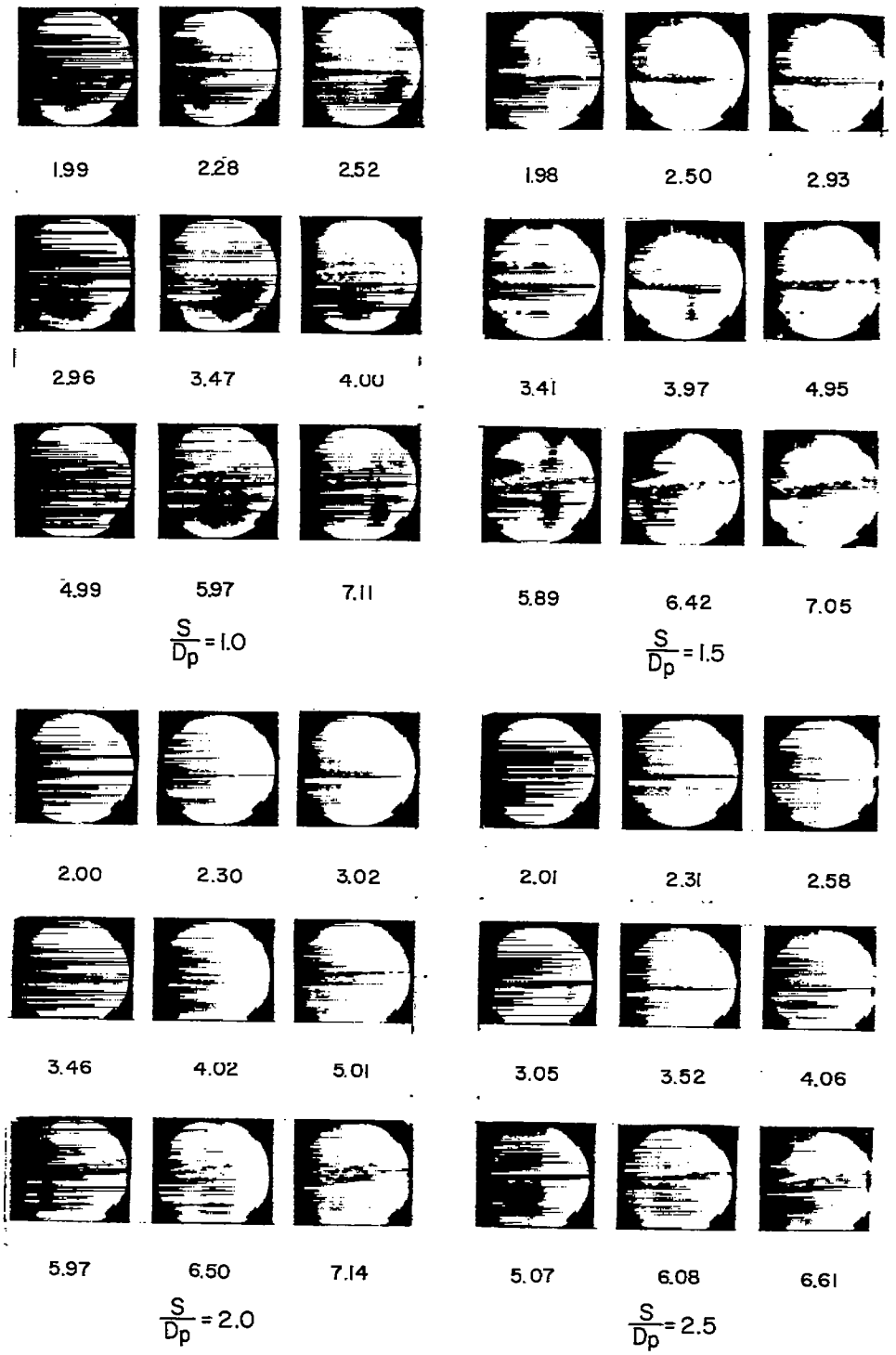

L-58-1682

(b) Schlieren photographs. Jet pressure ratio $p_{t,j}/p_{am}$ is indicated under each picture.

Figure 8.- Concluded.

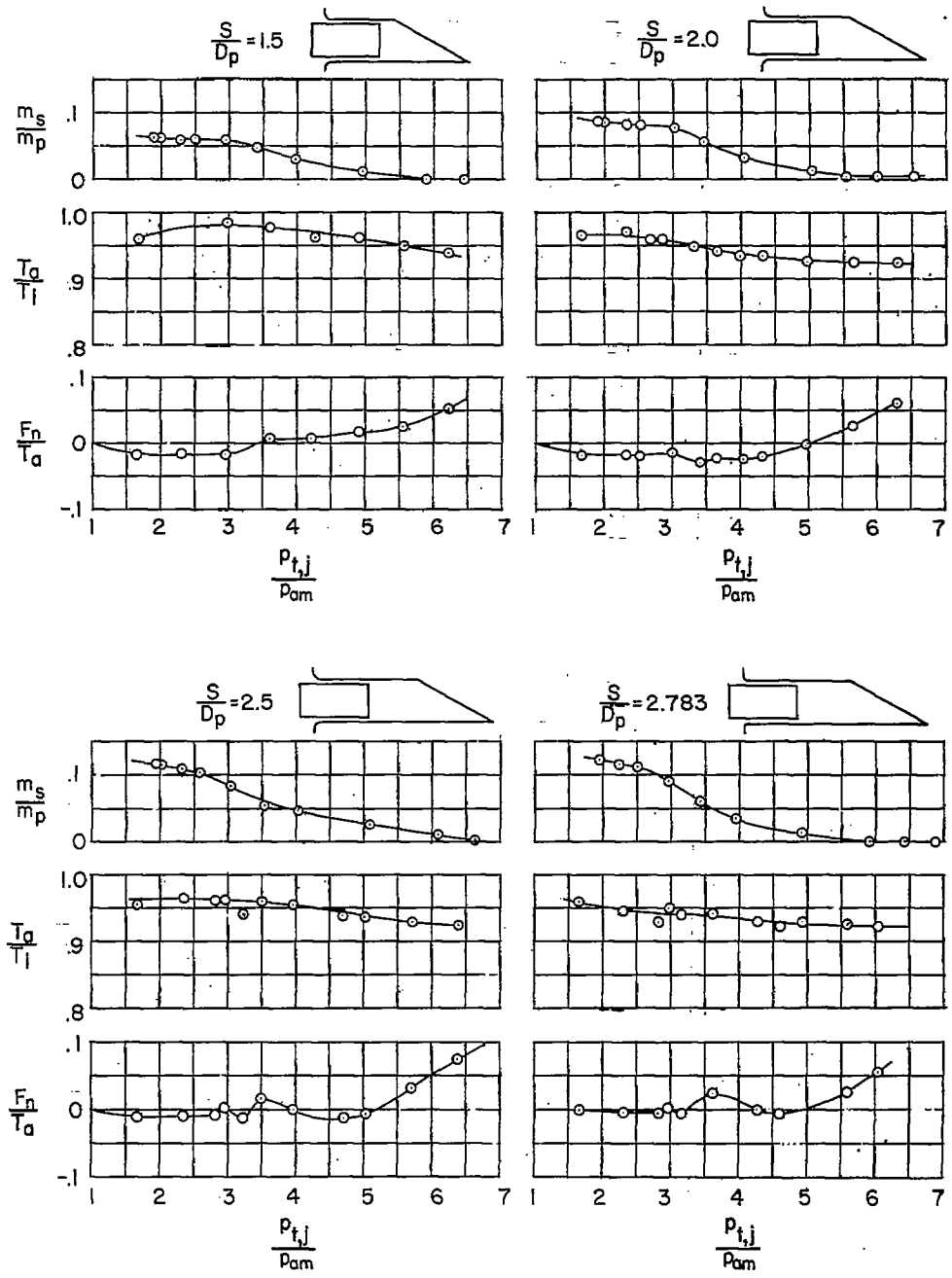

(a) Variation of m_s/m_p, T_a/T_i, and F_n/T_a with $p_{t,j}/p_{am}$.

Figure 9.- Ejectors with diameter ratio of 1.25 and unskewed primary nozzles. Shroud skew angle, 60°.

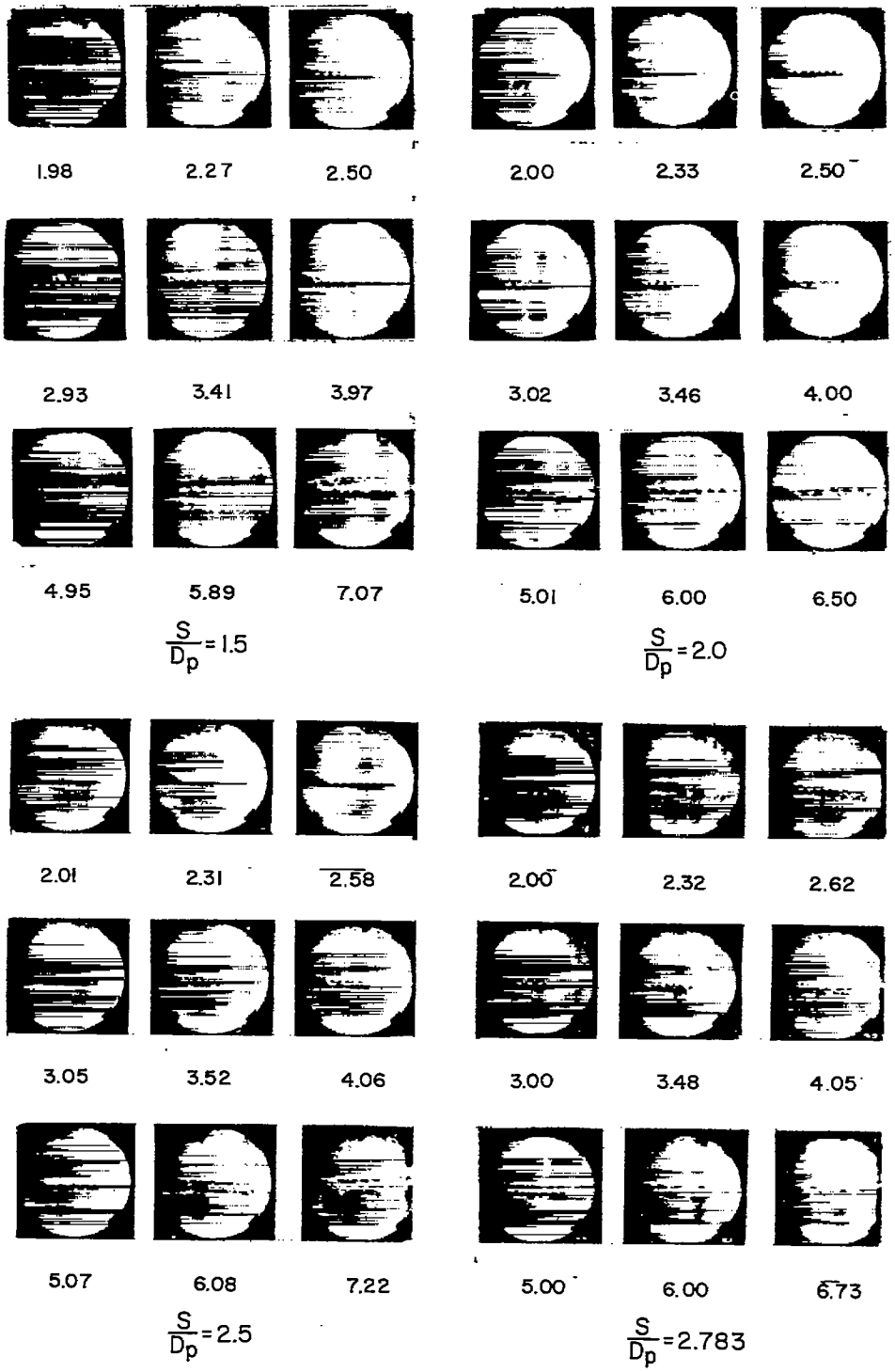

(b) Schlieren photographs. Jet pressure ratio $p_{t,j}/p_{am}$ is indicated under each picture. L-58-1683

Figure 9.- Concluded.

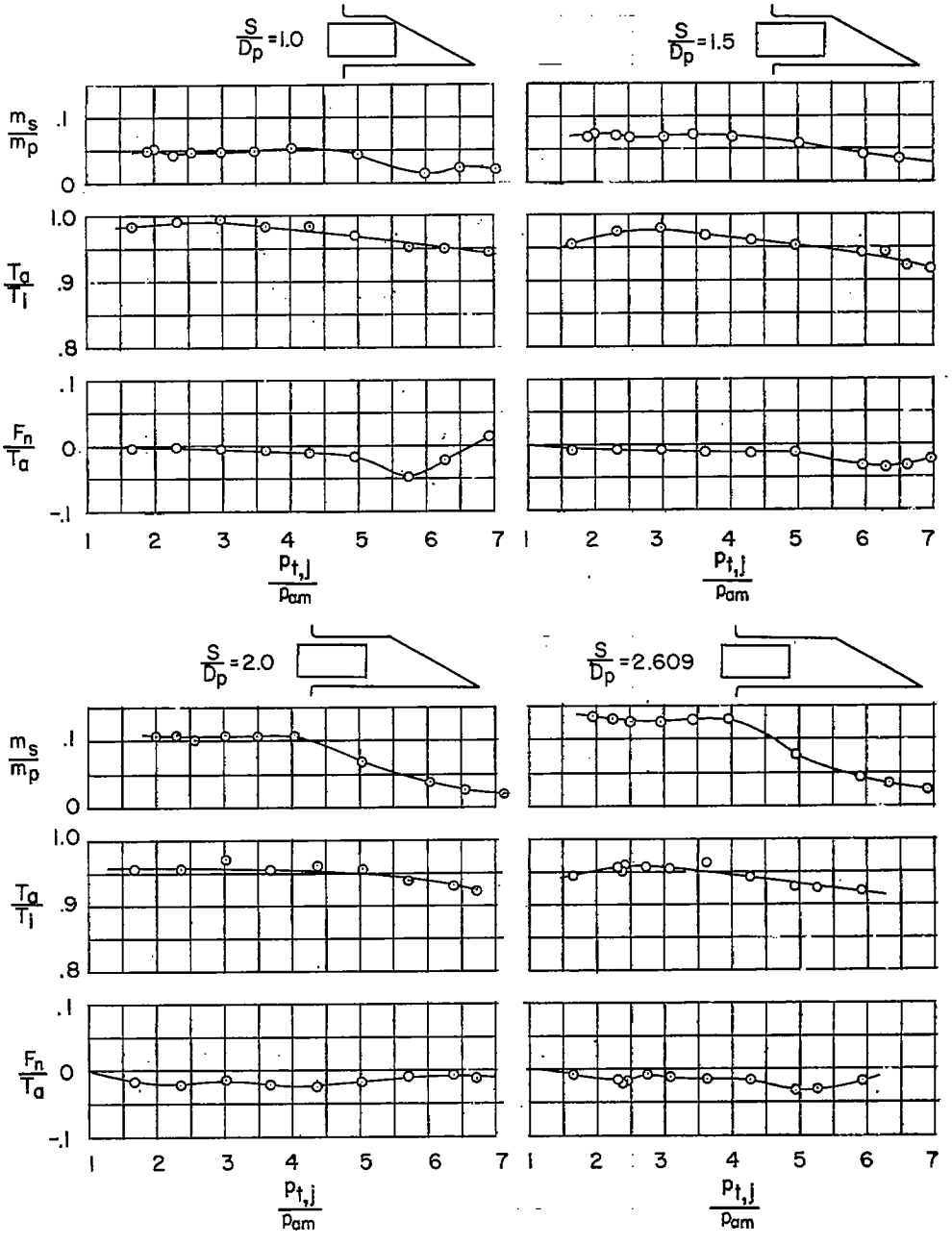

(a) Variation of m_s/m_p, T_a/T_i, and F_n/T_a with $p_{t,j}/p_{am}$.

Figure 10.- Ejectors with diameter ratio of 1.45 and unskewed primary nozzles. Shroud skew angle, 60°.

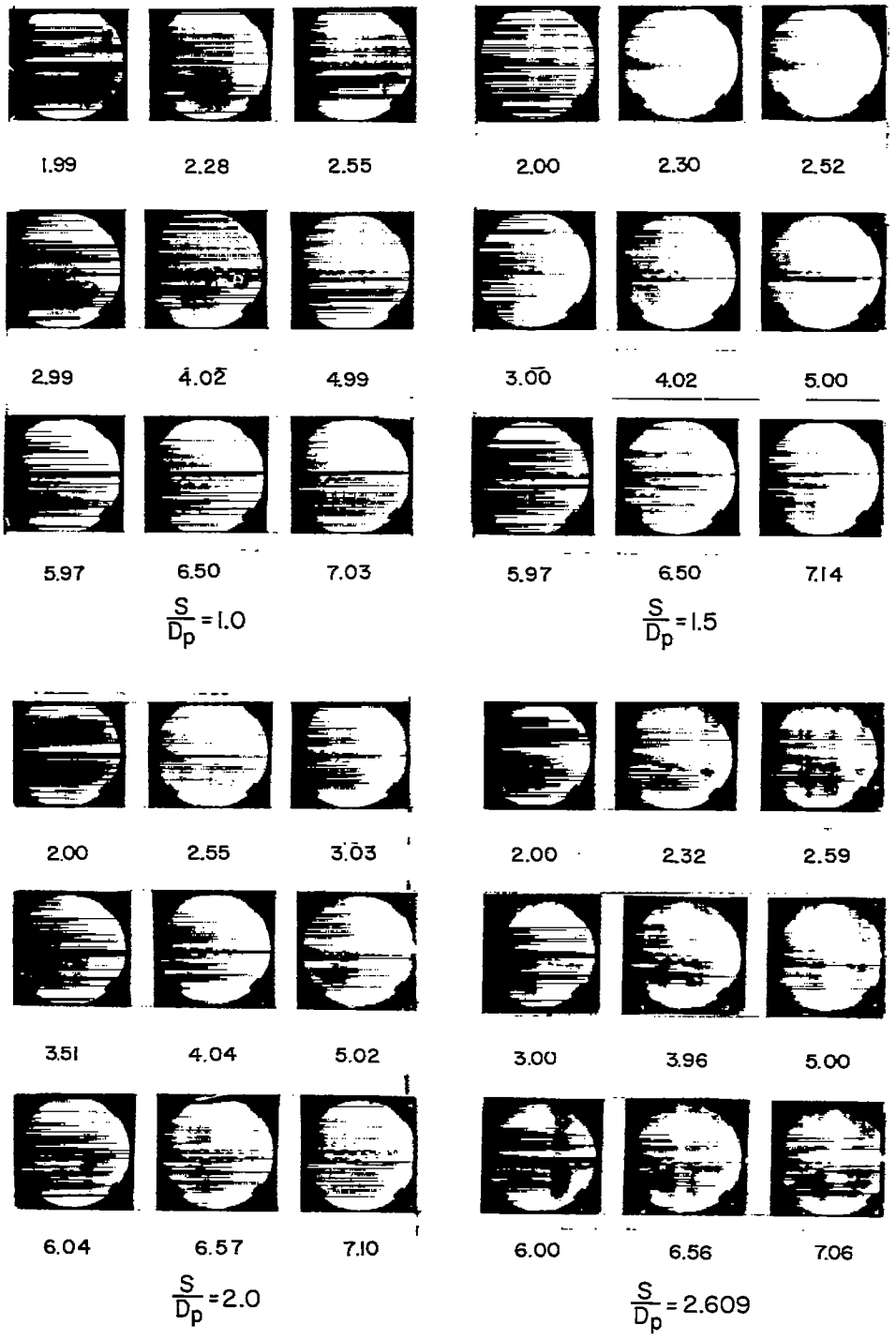

L-58-1684

(b) Schlieren photographs. Jet pressure ratio $p_{t,j}/p_{am}$ is indicated under each picture.

Figure 10.- Concluded.

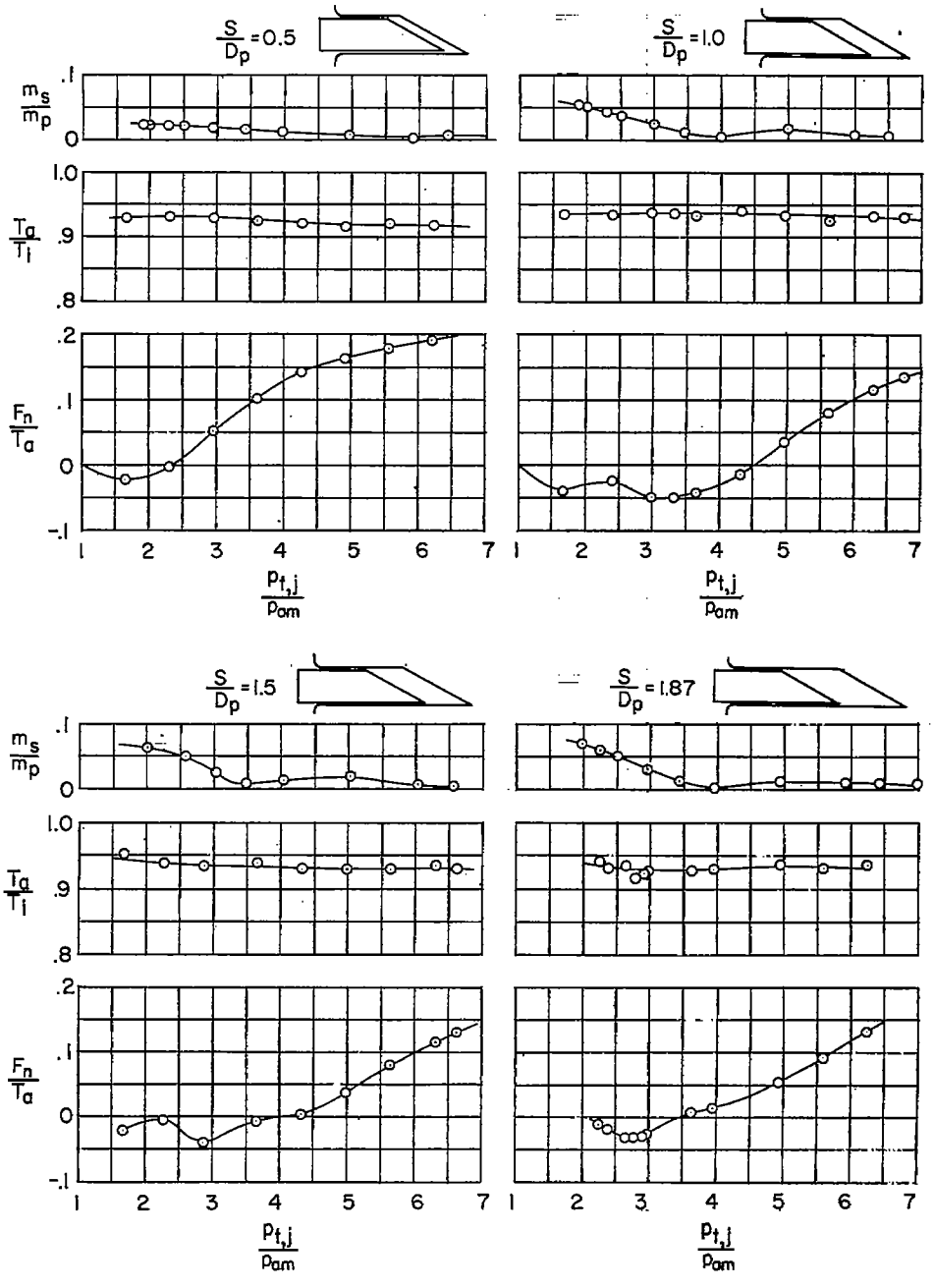

(a) Variation of m_s/m_p, T_a/T_i, and F_n/T_a with $p_{t,j}/p_{am}$.

Figure 11.- Ejectors with diameter ratio of 1.15 and skewed primary nozzles. Angles of skew, 60°.

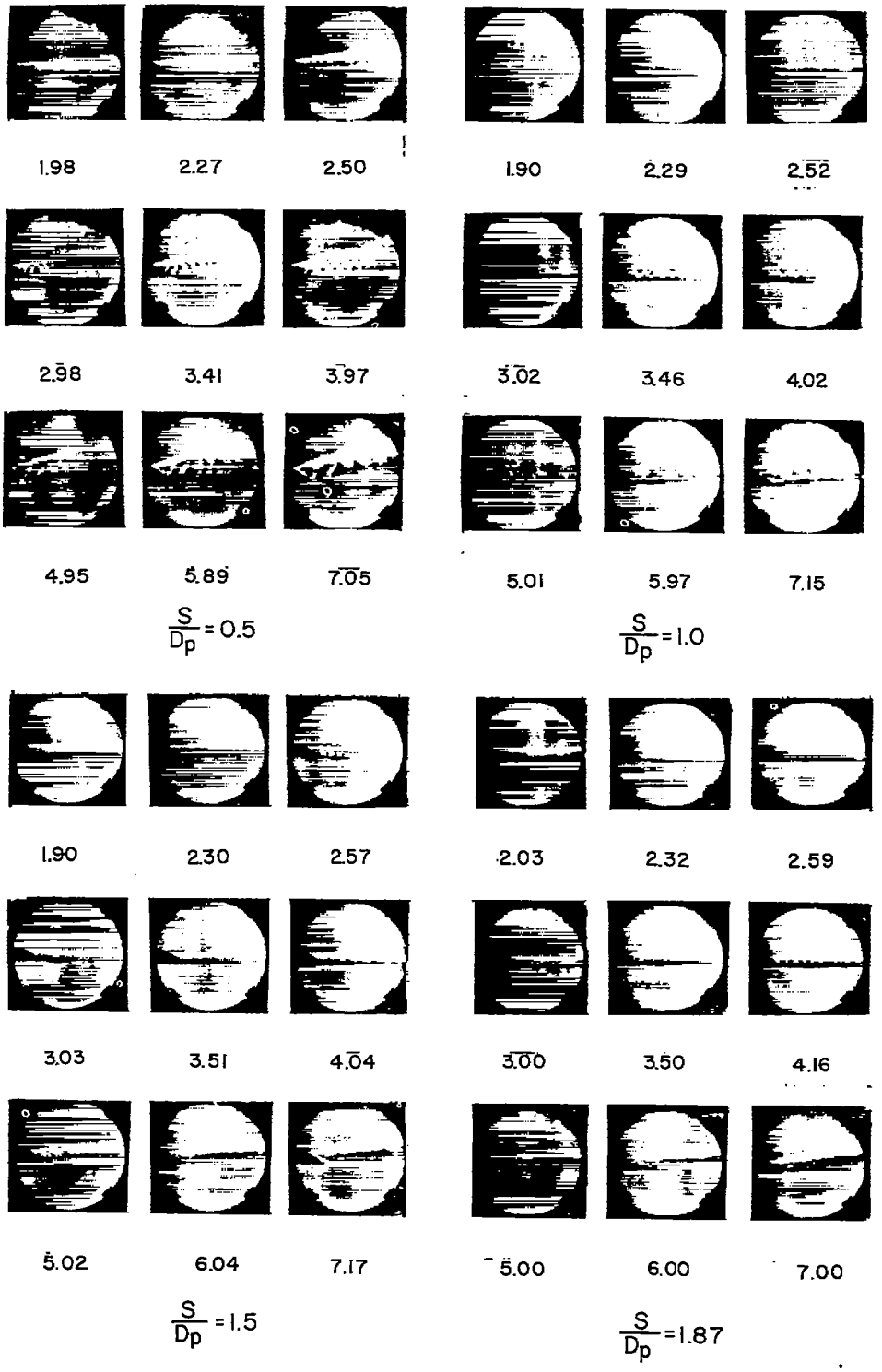

(b) Schlieren photographs. Jet pressure ratio $p_{t,j}/p_{am}$ is indicated under each picture. L-58-1685

Figure 11.- Concluded.

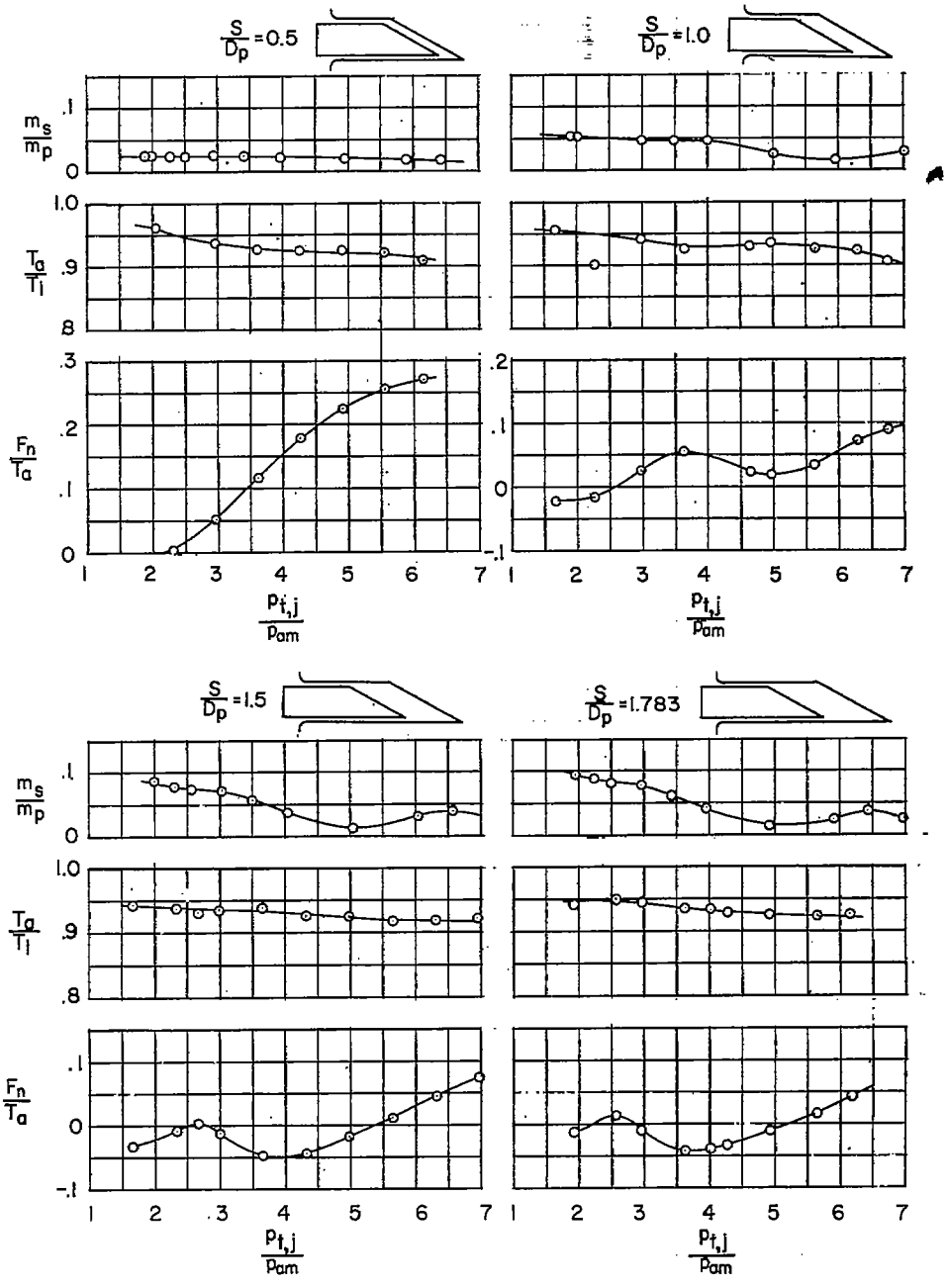

(a) Variation of m_s/m_p, T_a/T_i, and F_n/T_a with $p_{t,j}/p_{am}$.

Figure 12.- Ejectors with diameter ratio of 1.25 and skewed primary nozzles. Angles of skew, 60°.

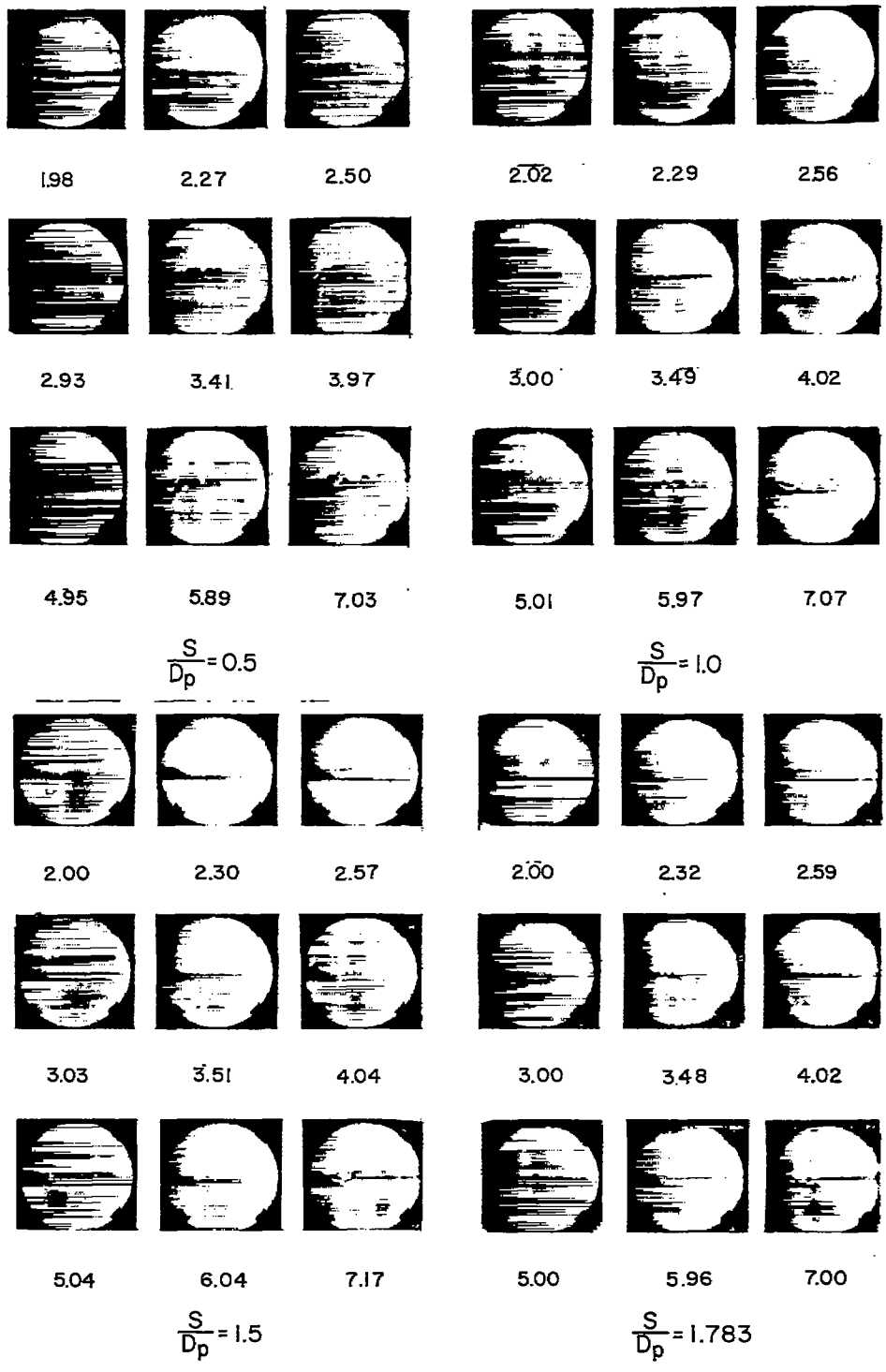

L-58-1686

(b) Schlieren photographs. Jet pressure ratio $p_{t,j}/p_{am}$ is indicated under each picture.

Figure 12.- Concluded.

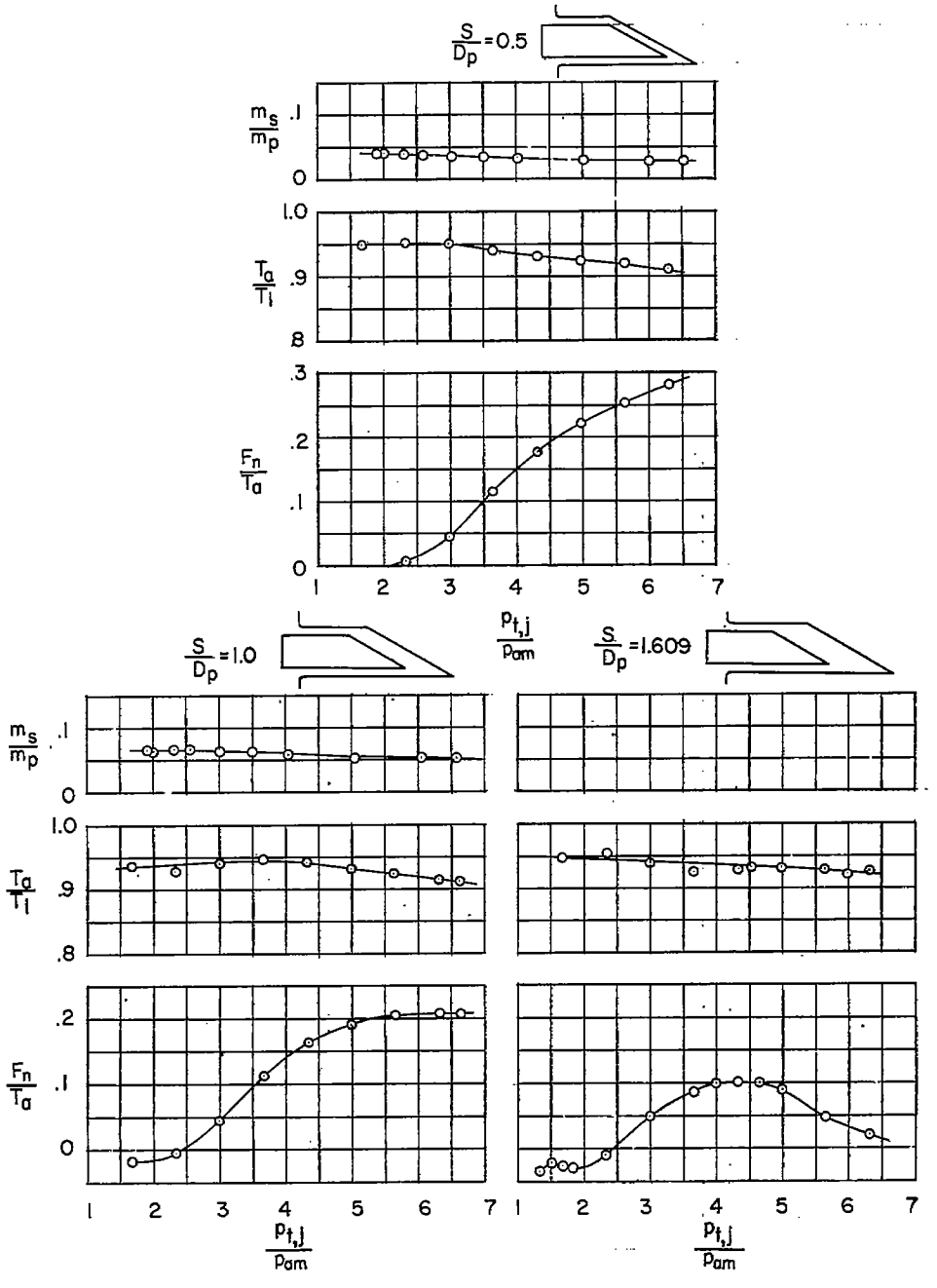

(a) Variation of m_s/m_p, T_a/T_i, and F_n/T_a with $p_{t,j}/p_{am}$.

Figure 13.- Ejectors with diameter ratio of 1.45 and skewed primary nozzles. Angles of skew, 60°.

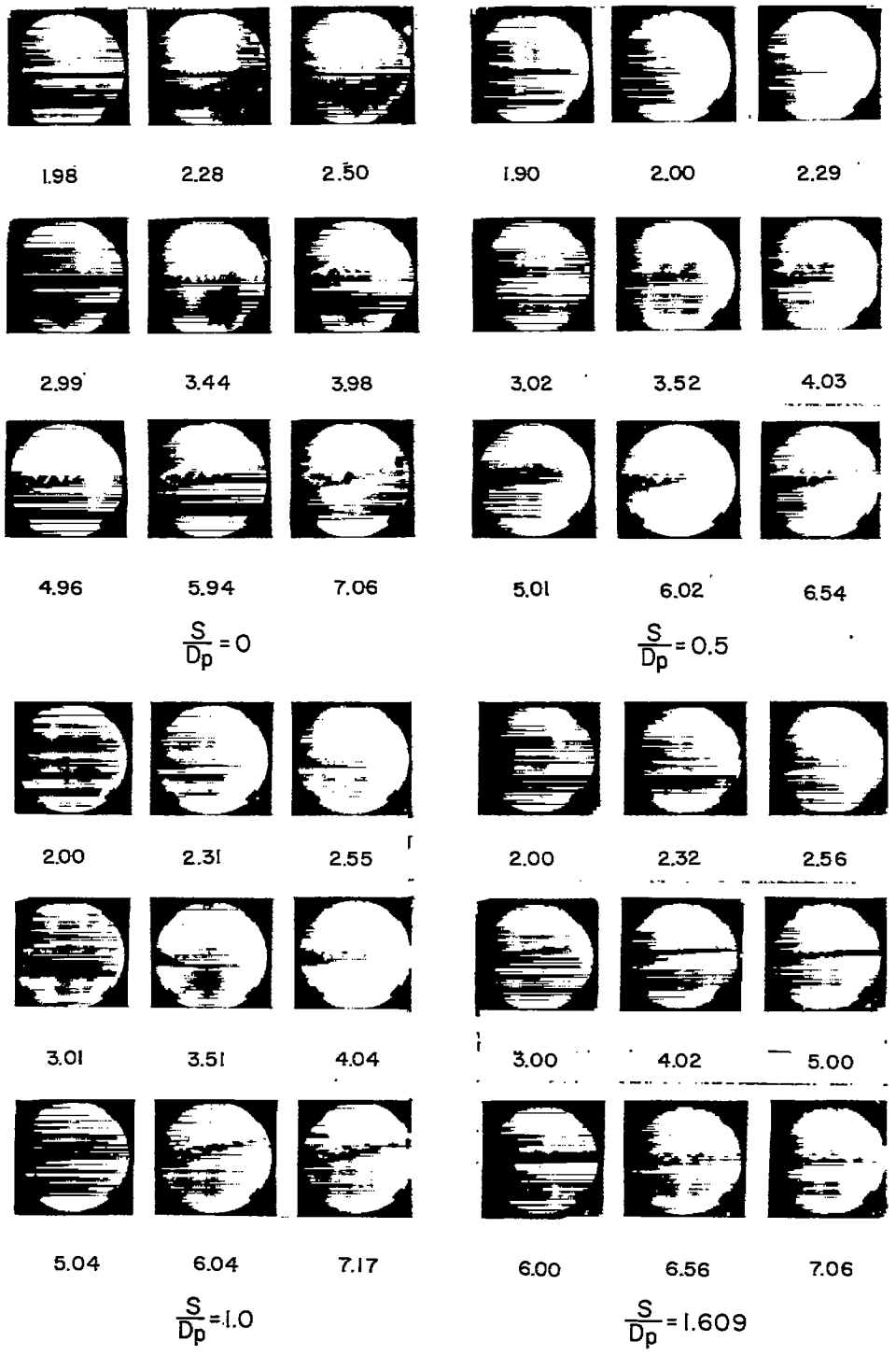

L-58-1687

(b) Schlieren photographs. Jet pressure ratio $p_{t,j}/p_{am}$ is indicated under each picture.

Figure 13.- Concluded.

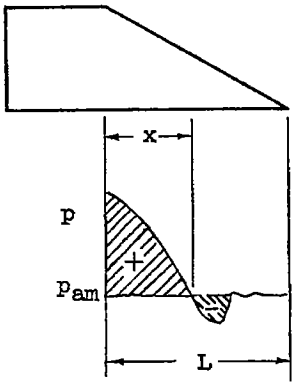

Typical pressure distribution

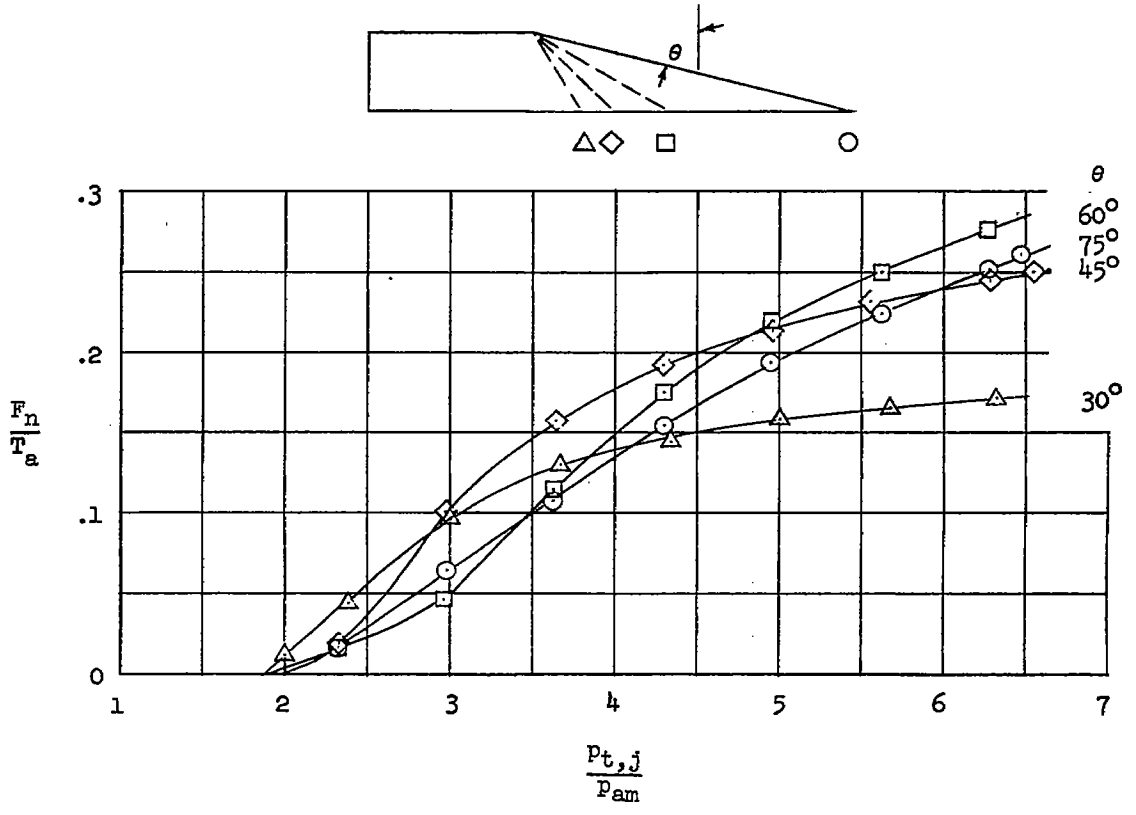

Figure 14.- Effect of angle of skew on F_n/T_a as a function of jet pressure ratio.

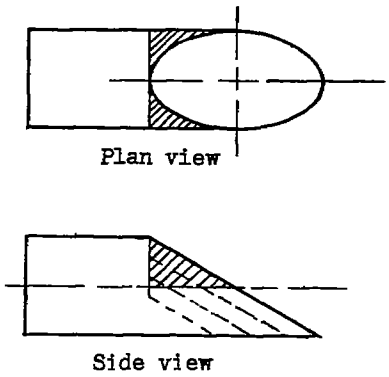

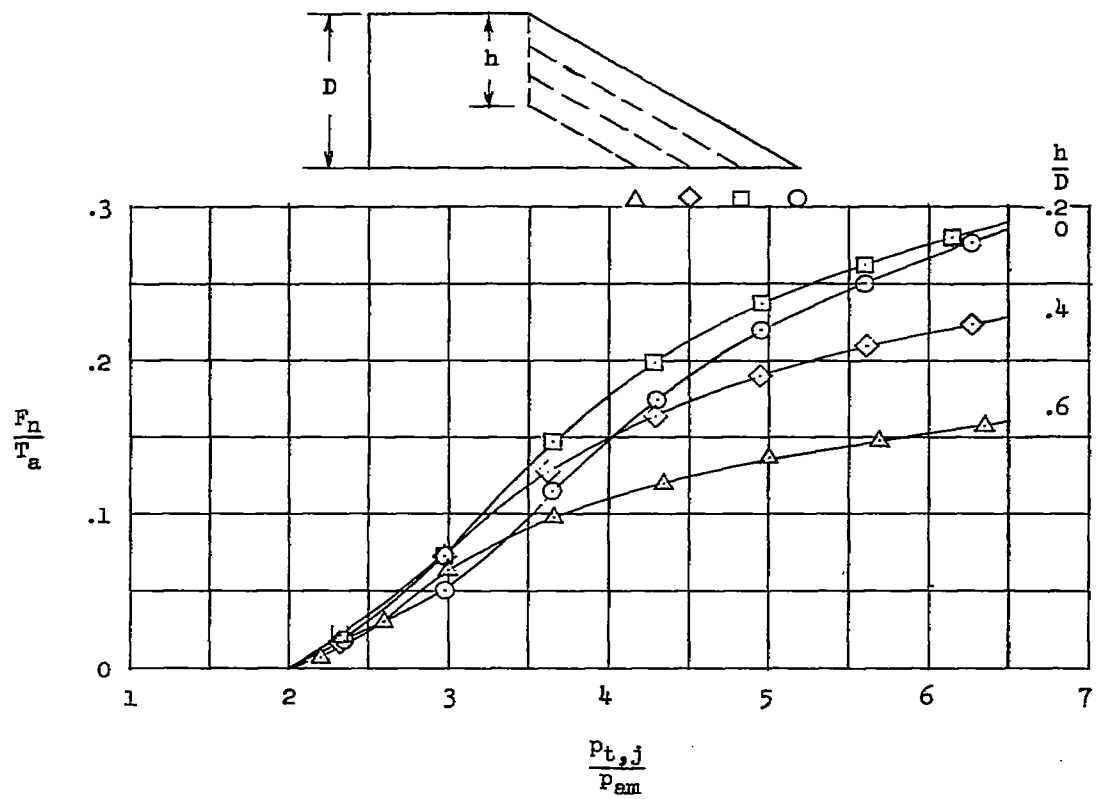

Figure 15.- Effect of indentation on F_n/T_a as a function of jet pressure ratio. Angles of skew, 60°.

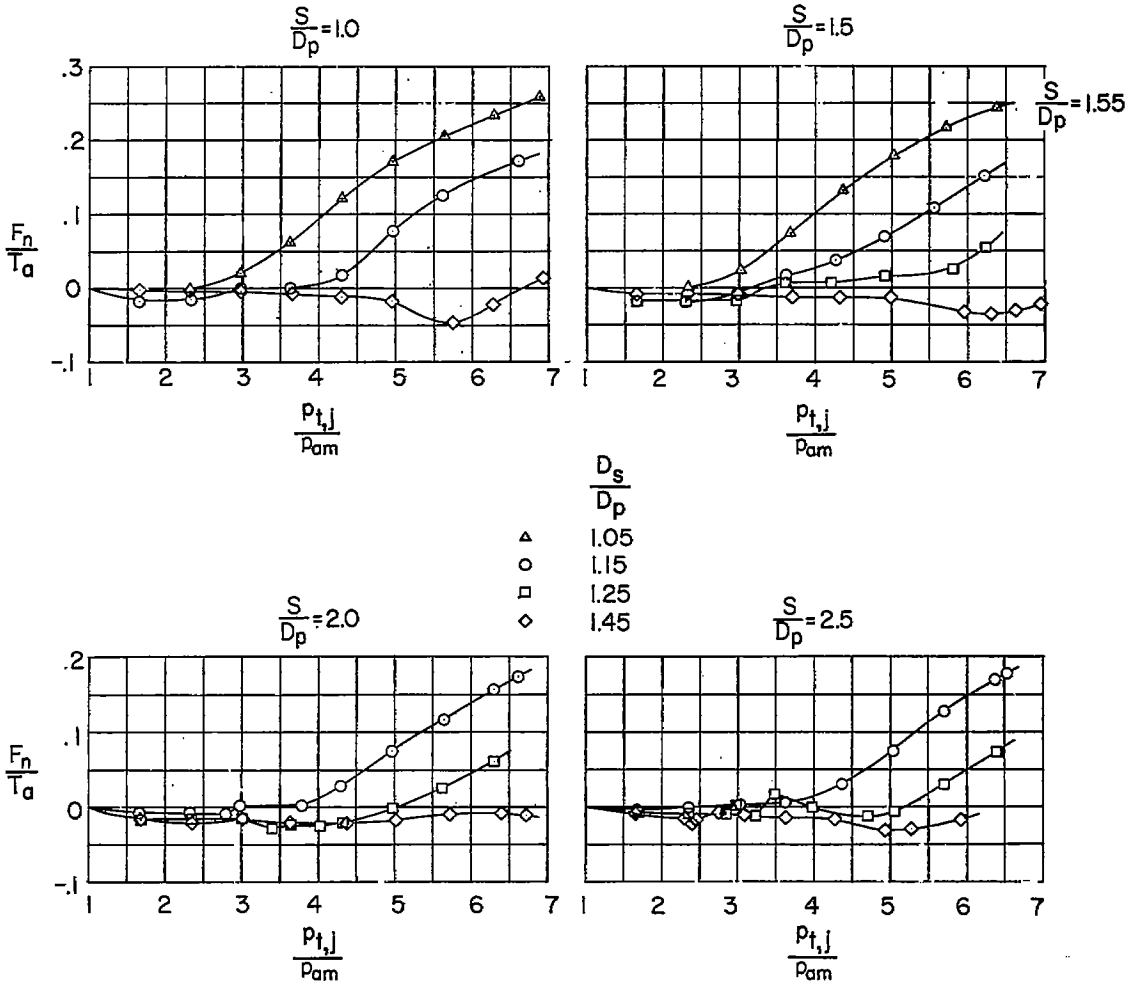

Figure 16.- Comparison of normal-force ratios for ejectors with unskewed primary nozzles. Diameter ratios and spacing ratios are as indicated.

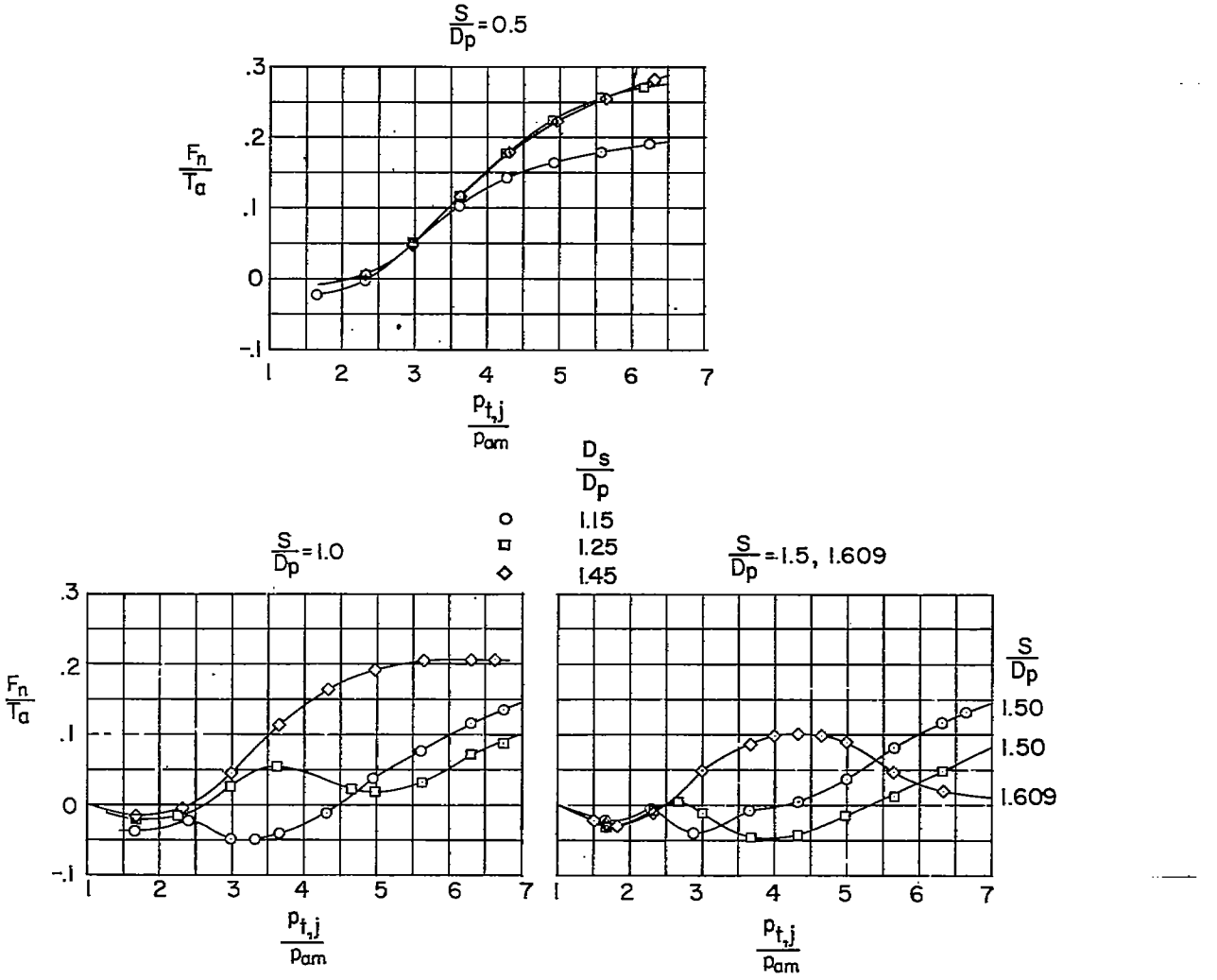

Figure 17.- Comparison of normal-force ratios for ejectors with skewed primary nozzles. Diameter ratios and spacing ratios are as indicated.

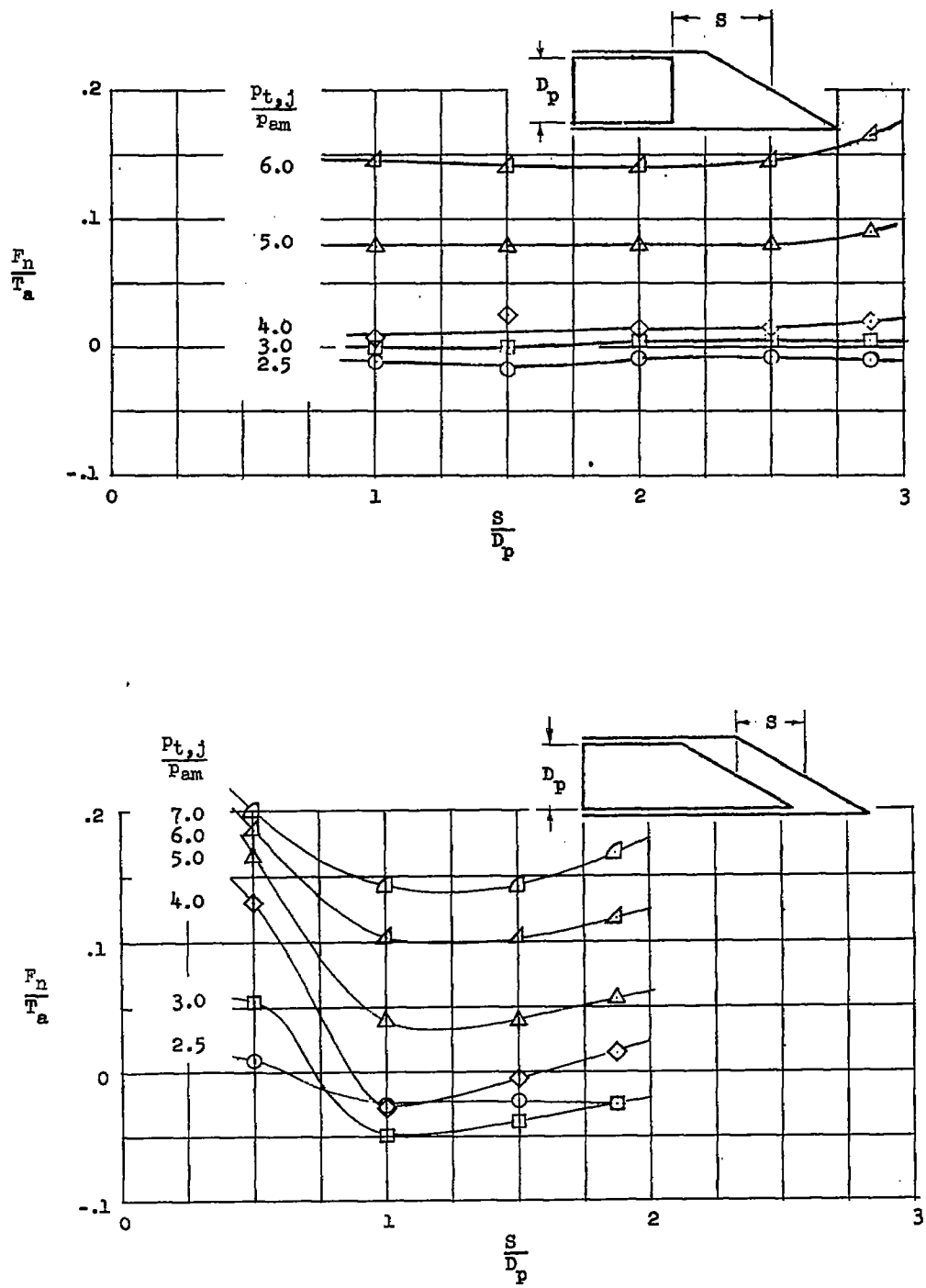

Figure 18.- Variation of normal-force ratio with spacing ratio for ejectors with diameter ratio of 1.15.

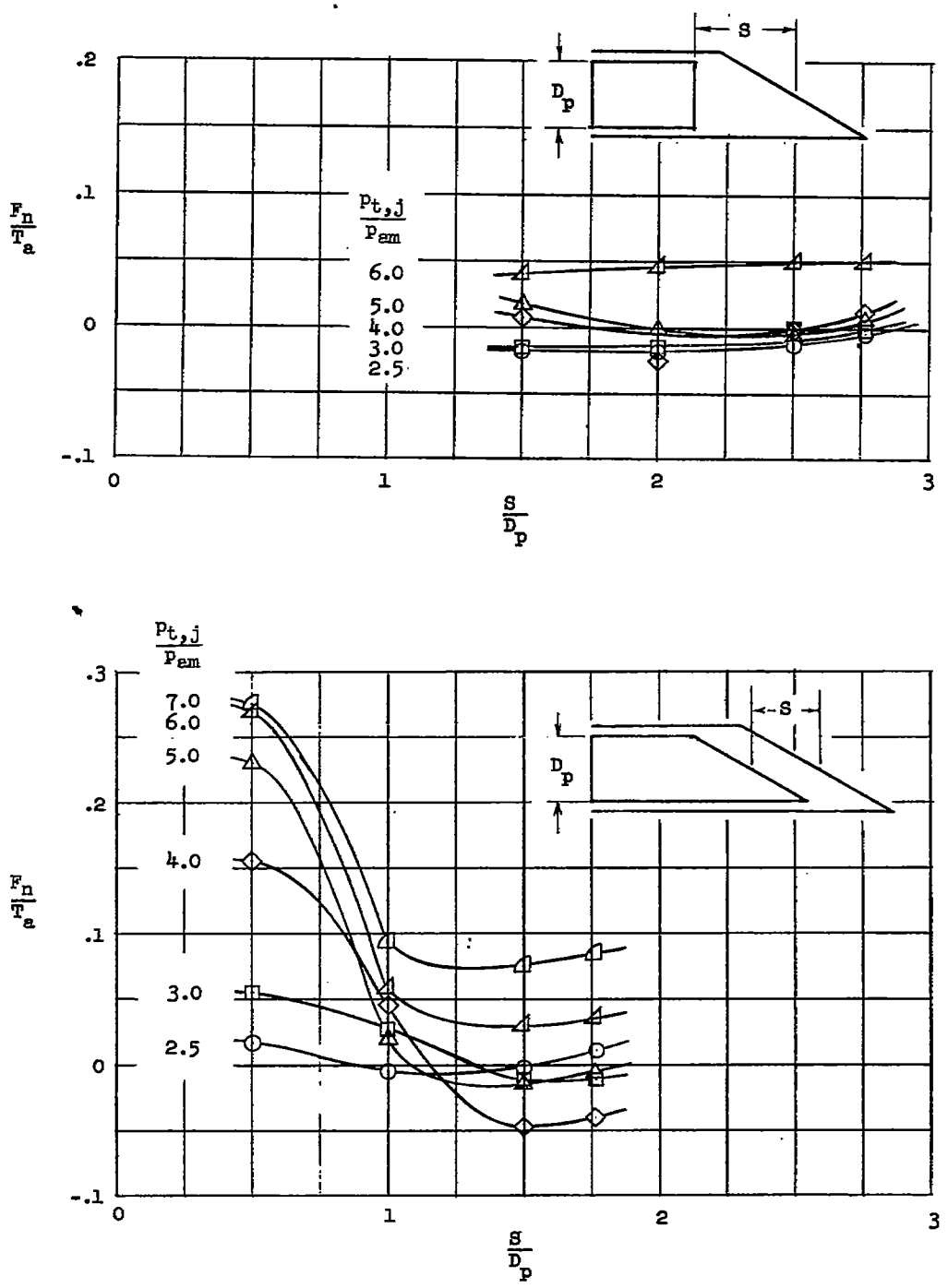

Figure 19.- Variation of normal-force ratio with spacing ratio for ejectors with diameter ratio of 1.25.

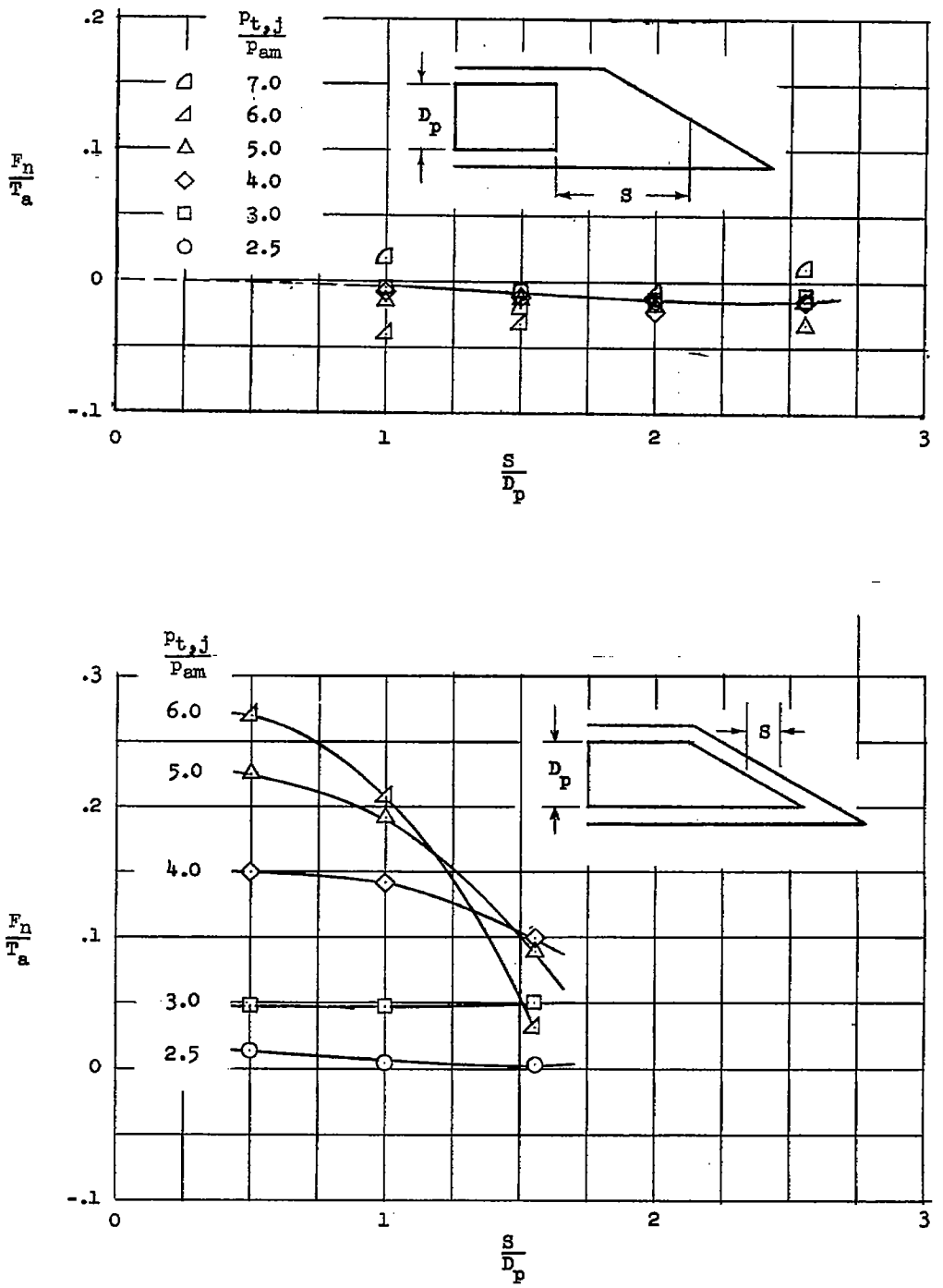

Figure 20.- Variation of normal-force ratio with spacing ratio for ejectors with diameter ratio of 1.45.